

Journal of Visualized Experiments

Management of respiratory motion artifacts in [18F]-fluorodeoxyglucose PET using an amplitude-based optimal respiratory gating algorithm --Manuscript Draft--

Article Type:	Invited Methods Article - JoVE Produced Video
Manuscript Number:	JoVE60258R4
Full Title:	Management of respiratory motion artifacts in [18F]-fluorodeoxyglucose PET using an amplitude-based optimal respiratory gating algorithm
Section/Category:	JoVE Cancer Research
Keywords:	Positron emission tomography; respiratory motion; correction; artifacts; quantification; lung cancer; Pancreatic cancer; liver lesions
Corresponding Author:	Erik H.J.G. Aarntzen, Ph.D, M.D. Radboud university medical center Nijmegen, Gelderland NETHERLANDS
Corresponding Author's Institution:	Radboud university medical center
Corresponding Author E-Mail:	Erik.Aarntzen@radboudumc.nl
Order of Authors:	Willem Grootjans Peter Kok Jurrian Butter Erik H.J.G. Aarntzen, Ph.D, M.D.
Additional Information:	
Question	Response
Please indicate whether this article will be Standard Access or Open Access.	Standard Access (US\$2,400)
Please indicate the city, state/province, and country where this article will be filmed . Please do not use abbreviations.	Nijmegen, Gelderland, The Netherlands

TITLE:

Management of Respiratory Motion Artefacts in ^{18}F -fluorodeoxyglucose Positron Emission Tomography using an Amplitude-Based Optimal Respiratory Gating Algorithm

AUTHORS & AFFILIATIONS:

Willem Grootjans¹, Peter Kok², Jurrian Butter², Erik Aarntzen²

¹Department of Radiology, Leiden University Medical Centre, Leiden, The Netherlands

²Department of Radiology and Nuclear medicine, Radboud university medical Centre, Nijmegen, The Netherlands

Corresponding author:

Willem Grootjans

W.Grootjans@lumc.nl

Peter Kok: Peter.Kok@radboudumc.nl

Jurrian Butter: Jurrian.Butter@radboudumc.nl

Erik Aarntzen: Erik.Aarntzen@radboudumc.nl

KEYWORDS:

Respiratory gating, Image quantification, Positron emission tomography, Non-small cell lung Cancer, Radiomics, Radiotherapy planning

SUMMARY:

Amplitude-based optimal respiratory gating (ORG) effectively removes respiratory-induced motion blurring from clinical ^{18}F -fluorodeoxyglucose (FDG) positron emission tomography (PET) images. Correction of FDG-PET images for these respiratory motion artefacts improves image quality, diagnostic and quantitative accuracy. Removal of respiratory motion artefacts is important for adequate clinical management of patients using PET.

ABSTRACT:

Positron emission tomography (PET) combined with X-ray computed tomography (CT) is an important molecular imaging platform that is required for accurate diagnosis and clinical staging of a variety of diseases. The advantage of PET imaging is the ability to visualize and quantify a myriad of biological processes in vivo with high sensitivity and accuracy. However, there are multiple factors that determine image quality and quantitative accuracy of PET images. One of the foremost factors influencing image quality in PET imaging of the thorax and upper abdomen is respiratory motion, resulting in respiration-induced motion blurring of anatomical structures. Correction of these artefacts is required for providing optimal image quality and quantitative accuracy of PET images.

Several respiratory gating techniques have been developed, typically relying on acquisition of a respiratory signal simultaneously with PET data. Based on the respiratory signal acquired, PET

data is selected for reconstruction of a motion-free image. Although these methods have been shown to effectively remove respiratory motion artefacts from PET images, the performance is dependent on the quality of the respiratory signal being acquired. In this study, the use of an amplitude-based optimal respiratory gating (ORG) algorithm is discussed. In contrast to many other respiratory gating algorithms, ORG permits the user to have control over image quality versus the amount of rejected motion in the reconstructed PET images. This is achieved by calculating an optimal amplitude range based on the acquired surrogate signal and a user-specified duty cycle (the percentage of PET data used for image reconstruction). The optimal amplitude range is defined as the smallest amplitude range still containing the amount of PET data required for image reconstruction. It was shown that ORG results in effective removal of respiration-induced image blurring in PET imaging of the thorax and upper abdomen, resulting in improved image quality and quantitative accuracy.

INTRODUCTION:

Positron Emission Tomography (PET) in combination with X-ray computed tomography (CT) is a widely accepted imaging tool in clinical practice for accurate diagnosis and clinical staging of a variety of diseases¹. The advantage of PET imaging is the ability to visualize and quantify a myriad of biological processes in vivo with high sensitivity and accuracy². This is achieved through intravenously administering a radioactively labelled compound, also known as a radiotracer, to the patient. Depending on the radiotracer being used, tissue characteristics such as glucose metabolism, cellular proliferation, degree of hypoxia, amino acid transport, and expression of proteins and receptors, can be visualized and quantified².

Although several radiotracers have been developed, validated, and used in clinical practice, the radioactive glucose analogue ¹⁸F-fluorodeoxyglucose (FDG) is the most widely used radiotracer in clinical practice. Given that FDG predominantly accumulates in cells with an elevated glycolytic rate (i.e., cells with elevated glucose uptake and conversion to pyruvate for energy production), it is possible to discriminate tissues with different metabolic states. Similar to glucose, the first step of FDG uptake is transport from the extra-cellular space over the plasma membrane to the intra-cellular space, which is facilitated by glucose transporters (GLUT)³. Once the FDG is in the intra-cellular space, phosphorylation by hexokinases will result in the generation of FDG-6-phosphate. However, in contrast to glucose-6-phosphate, FDG-6-phosphate cannot enter the Krebs cycle for further aerobic dissimilation due to the absence of a hydroxyl (OH) group at the second (2') carbon position. Given that the reverse reaction, the dephosphorylation of FDG-6-phosphate back to FDG, hardly occurs in most tissues, the FDG-6-phosphate is trapped intracellularly³. Therefore, the degree of FDG uptake is dependent on the expression of the GLUT (in particular GLUT1 and GLUT3) on the plasma membrane, and the intracellular enzymatic activity of hexokinases. The concept of this continuous uptake and trapping of FDG is referred to as metabolic trapping. The fact that FDG preferentially accumulates in tissues with an elevated metabolic activity is shown in **Figure 1a**, demonstrating the physiological distribution of FDG in a patient. This FDG-PET image shows higher uptake in heart, brain, and liver tissues, which are known to be metabolically active organs under normal conditions.

The high sensitivity for detecting differences in the metabolic state of tissues makes FDG an

excellent radiotracer for discriminating normal from diseased tissues, given that an altered metabolism is an important hallmark for many diseases. This is readily depicted in **Figure 1b**, showing an FDG-PET image of a patient with stage IV non-small cell lung cancer (NSCLC). There is increased uptake in the primary tumor as well as in metastatic lesions. In addition to visualization, quantification of radiotracer uptake plays an important role in clinical management of patients. Quantitative indices derived from PET images reflecting the degree of radiotracer uptake, such as the standardized uptake value (SUV), metabolic volumes, and total lesion glycolysis (TLG), can be used to provide important prognostic information and measure treatment response for different patient groups⁴⁻⁶. In this regard, FDG-PET imaging is increasingly being used to personalize radiotherapy and systemic treatment in oncology patients⁷. Furthermore, the use of FDG-PET for monitoring acute treatment induced toxicity, such as radiation induced esophagitis⁸, pneumonitis⁹ and systemic inflammatory responses¹⁰, has been described and provides important information for making image-guided treatment decisions.

Given the important role of PET for clinical management of patients, image quality and quantitative accuracy is important for appropriately guiding treatment decisions based on PET images. However, there are numerous technical factors that can compromise quantitative accuracy of PET images¹¹. An important factor that can significantly influence image quantification in PET is related to the longer acquisition times of PET compared to other radiological imaging modalities, typically several minutes per bed position. As a consequence, patients are usually instructed to breath freely during PET imaging. The result is that PET images suffer from respiratory induced motion, which can lead to significant blurring of organs located within the thorax and upper abdomen. This respiratory-induced motion blurring can significantly impair adequate visualization and quantitative accuracy of radiotracer uptake, which can affect clinical management of patients when using PET images for diagnosis and staging, target volume definition for radiation treatment planning applications, and monitoring of therapy response¹².

Several respiratory gating methods have been developed in an attempt to correct PET images for respiratory motion artefacts¹³. These methods can be categorized into prospective, retrospective, and data-driven gating strategies. Prospective and retrospective respiratory gating techniques typically rely on the acquisition of a respiratory surrogate signal during PET imaging¹⁴. These respiratory surrogate signals are used to track and monitor the patient's respiratory cycle. Examples of respiratory tracking devices are detection of chest wall excursion using pressure sensors¹² or optical tracking systems (e.g., video cameras)¹⁵, thermocouples to measure the temperature of breathed air¹⁶, and spirometers to measure airflow and thereby indirectly estimating volume changes in the patient's lungs¹⁷.

Respiratory gating is then typically accomplished by continuously and simultaneously recording a surrogate signal (designated $S(t)$), with the PET data during image acquisition. Using the surrogate signal acquired, PET data corresponding to a particular respiratory phase or amplitude range (amplitude-based gating) can be selected^{12,13,18}. Phase-based gating is performed by dividing each respiratory cycle into a fixed number of gates, as depicted in **Figure 2a**. Respiratory gating is then performed by selecting data acquired at a particular phase during the patient's respiratory cycle to be used for image reconstruction. Similarly, amplitude-based gating relies on

defining an amplitude range of the respiratory signal, as shown in **Figure 2b**. When the value of the respiratory signal falls within the set amplitude range, the corresponding PET listmode data will be used for image reconstruction. For retrospective gating approaches, all data is collected and re-binning of the PET data is performed after image acquisition. Although prospective respiratory gating methods use the same concepts as retrospective gating approaches for re-binning of PET data, these methods rely on collecting data prospectively during image acquisition. When a sufficient amount of PET data is collected, image acquisition will be finalized. The difficulty of such prospective and retrospective gating approaches is maintaining acceptable image quality without significantly prolonging image acquisition times when irregular breathing¹³. In this regard, phase-based respiratory gating methods are particularly sensitive to irregular breathing patterns^{13,19}, where significant amounts of PET data can be discarded due to rejection of inappropriate triggers, resulting in considerable reduction of image quality or unacceptable lengthening of image acquisition time. Additionally, when inappropriate triggers are accepted, the performance of the respiratory gating algorithm and thereby the effectiveness of motion rejection from the PET images can be reduced due to the fact that respiratory gates are defined at different phases of the respiratory cycle, as depicted in **Figure 2a**. Indeed, it has been reported that amplitude-based respiratory gating is more stable than phase-based approaches in case of irregularities in the respiratory signal¹³. Though amplitude-based respiratory gating algorithms are more robust in the presence of irregular breathing frequencies, these algorithms are more sensitive to baseline drifting of the respiratory signal. Drifting of the baseline signal can occur due to numerous reasons when the patient's muscle tension (i.e., transition of a patient into a more relaxed state during image acquisition) or breathing pattern changes. In order to prevent such baseline drifting of the signal, care should be taken to securely attach tracking sensors to the patient and perform regular monitoring of the respiratory signal.

Although these problems are known, traditional respiratory gating algorithms permit limited control over image quality and usually require significant lengthening of image acquisition time or increased amounts of radiotracer to be administered to the patient. These factors resulted in limited adoption of such protocols in clinical routine. In order to circumvent these problems related to the variable quality of the respiratory gated images, a specific type of amplitude-based gating algorithm, also known as optimal respiratory gating (ORG), has been proposed¹⁸. Respiratory gating with ORG permits the user to specify image quality of the respiratory gated images by providing a duty cycle as input to the algorithm. The duty cycle is defined as a percentage of the acquired PET list-mode data that is used for image reconstruction. In contrast to many other respiratory gating algorithms, this concept permits the user to directly determine image quality of the reconstructed PET images. Based on the duty cycle specified, an optimal amplitude range is calculated, which takes the specific characteristics of the entire respiratory surrogate signal into account¹⁸. The optimal amplitude range for a specific duty cycle will be calculated by starting with a selection of different values for the lower amplitude limit, designated (L), of the respiratory signal. For each selected lower limit, the upper amplitude limit, designated (U), is adjusted in such a way that the sum of the selected PET data, defined as data acquired when the respiratory signal falls within the amplitude range ($L < S(t) < U$), is equal to the specified duty cycle. For example, for a duty cycle of 50% and six minutes of acquired PET listmode data, the amplitude range is adapted to include at three minutes (50%) of PET data. The

optimal amplitude range (W) is defined as the smallest amplitude range used for respiratory gating that still contains the required amount of PET data (i.e., $\text{ArgMax}([U-L])$), as depicted in **Figure 2c**¹². Thus, by specifying the duty cycle, the user makes a trade-off between the amount of noise and the degree of residual motion residing in the ORG PET images. Lowering the duty cycle will increase the amount of noise, though this will also reduce the amount of residual motion in the PET images (and vice versa). Although the concepts and effects of ORG have been described in previous reports, the purpose of this manuscript is to provide clinicians with details on the specific protocols when using ORG in clinical practice. Therefore, the use of ORG in a clinical imaging protocol is described. Several practical aspects, including patient preparation, image acquisition and reconstruction protocols will be provided. Furthermore, the manuscript will cover the user interface of the ORG software and specific choices that can be made when performing respiratory gating during PET imaging. Lastly, the effect of ORG on lesion detectability and image quantification, as shown in previous studies, are discussed.

PROTOCOL:

All procedures performed involving human participants were in accordance with the ethical standards of the internal review board (IRB) of the Radboud university medical center and with the 1964 Helsinki declaration and its later amendments or comparable ethical standards. The ORG algorithm is a vendor specific product and is available on the Siemens Biograph mCT PET/CT scanner family and newer PET/CT models.

1. Patient preparation

1.1. Patient anamnesis

1.1.1 Check the patient's name and date of birth. Inclusion criteria are similar to routine non-gated PET scanning. No additional in- or exclusion criteria are required.

1.1.2 Check the label delivered with the syringe containing the radiotracer (name, date of birth and amount of activity).

NOTE: The amount of activity administered to the patient is dependent on the patient's body mass and can vary between institutions. (in this protocol an amount of 3.2 MBq/kg is suggested).

1.1.3 Ensure that the clinical information on the application form is correct by interviewing the patient. Ask the patient whether there were any recent relevant changes in treatment or medication.

1.1.4 Ask the patient whether he or she has diabetes mellitus (DM). In case the patient has DM, ask whether he or she followed appropriate preparation (i.e., no administration of short working insulin less than 4 hours prior to the PET scan, or use of blood glucose lowering agents (such as metformin)).

221 1.1.5 Ask the patient whether he or she has any allergies or uses anticoagulants.

222
223 1.1.6 Measure the patient's blood glucose by applying a drop of blood obtained by pricking the
224 side of the fingertip of the patient on a dedicated test strip (the serum glucose should not exceed
225 11.0 mmol/L).

226
227 1.1.7 Explain the patient preparation and imaging procedures to the patient.

228 229 1.2. Administration of the radiotracer

230
231 1.2.1. Secure venous access to the patient by inserting a peripheral venous cannula in one of
232 the antecubital veins.

233
234 1.2.2. Attach a three way stop cock system with Luer lock to a 20 mL syringe containing saline
235 (this is the secondary syringe).

236
237 1.2.3. Flush the three way stop cock system with saline (for the purpose of deaeration).

238
239 1.2.4. Attach the three way stop cock with syringe to the end of the venous cannula.

240
241 1.2.5. Check whether the venous cannula is patent by carefully flushing 10 mL of saline through
242 the cannula (ask the patient whether he or she has any complaints during flushing).

243
244 1.2.6. Turn the valves of the three way stop cock so that the flow direction of fluid through the
245 system runs from the syringe containing the radiotracer to the peripheral venous cannula.
246 Administer the radiotracer by slowly pushing the plunger of the syringe (the syringe containing
247 the tracer is placed in a special lead shielded container).

248
249 1.2.7. Turn the valves of the three way stop cock in such a way that the syringe containing saline
250 is connected to the primary syringe (that contained the radiotracer) and flush the syringe to rinse
251 any residual radiotracer from the syringe.

252
253 1.2.8. Turn the valves of the three way stop cock and push the plunger of the primary syringe to
254 administer any residual radiotracer remaining in the syringe to the patient.

255
256 1.2.9. Repeat step 1.2.7. and 1.2.8. three times.

257
258 1.2.10. Remove the primary syringe and administer through the venous cannula 0.5 mg/Kg of
259 furosemide (with a maximum amount of 10 mg).

260 261 1.3. Patient incubation

262
263 1.3.1. Let the patient rest in a comfortable position for 50 minutes.

265 1.3.2. After 50 minutes, instruct the patient to void their bladder.

266
267 1.3.3. At 55 minutes, escort the patient to the scanner and position the patient supine with the
268 arms up on the scanner bed. Use appropriate arm support to make it as comfortable as possible
269 for the patient. If the patient is not able to elevate his or her arms, scanning can be performed
270 with the arms position alongside the patient.

271
272 1.3.4. Observe the patient's breathing pattern and secure the respiratory belt around the
273 patient's thorax (usually, the position just beneath the rib cage is optimal). Ensure that the sensor
274 is placed at a location where abdominal wall excursion is identified after visual inspection (usually
275 5-7 cm from the midline). Secure the belt around the patient by using the Velcro-based closing
276 system.

277
278 1.3.5. Check on the scanner display whether the respiratory signal remains within bounds of the
279 minimum and maximum range (if the respiratory signal is clipping, fasten or tighten the belt
280 appropriately).

281
282 1.3.6. Tip: Make sure the belt is fastened tight enough around the patient's chest. Given that
283 patients enter a more relaxed state after some time, the respiratory signal tends to drop (baseline
284 drift of the signal). This prevents the signal from going out of bounds, thus maintaining a high
285 quality of surrogate signal that is being used for respiratory gating.

286
287 1.3.7. Start scanning at 60 minutes after incubation time.

288 289 **2. Image acquisition and reconstruction**

290 291 **2.1 Protocol selection**

292
293 2.1.1. Select the whole-body protocol on the scanner. This can be done by moving the cursor
294 over the appropriate protocol category (indicated by the circles next to the patient icon in the
295 examination card), and click on the appropriate protocol (**Figure 3**).

296
297 2.1.2. The ORG acquisition protocol will start with a scout scan (topogram) of the patient. To
298 initiate acquisition of the topogram, press the scanner start key (yellow round key with a
299 radiation sign) on the scanner control box (**Figure 4**). To halt or abort acquisition of the topogram,
300 press the suspend or stop key respectively.

301
302 2.1.3. Start by planning the PET bed positions on the topogram. This can be done by clicking the
303 left mouse button on the topogram and setting the scan range.

304
305 2.1.4. Select the bed positions which to be corrected for respiratory motion (**Figure 5**).

306
307 NOTE: These are the 'gated' bed positions that cover the thorax. The 'gated' bed positions are
308 recorded in listmode. Depending on the clinical indication, bed positions covering the upper

abdomen can also be gated (for example when imaging is indicated for liver or pancreatic lesions). For the non-gated bed positions, it is only necessary to record the sinograms for image reconstruction.

2.1.5. Set image recording time for the PET bed positions (**Figure 6**).

NOTE: Depending on the amount of injected activity, scan duration of the bed positions has to be adapted to yield sufficient image quality. Depending on the recording time of the non-gated bed positions and the duty cycle being used, the recording time of the gated bed position is determined. For example, for a duty cycle of 35%, lengthening the scan by factor 3 yields approximately similar statistics for gated and non-gated bed positions. Suggested imaging protocol at the Radboud University Medical Center is a recording time for non-gated bed positions of 2 minutes, whilst for gated bed positions recording time is 6 minutes using a duty cycle of 35%

2.1.6. After setting up the acquisition parameters, press and hold the start key (yellow round button with a radiation sign) on the scanner control box and wait until the scanner bed has moved back to the starting position. Press the start key again to acquire a low dose CT scan from the patient (head to feet). After acquiring the CT scan, press the start key to initiate the PET scan.

2.1.7. During image acquisition, regularly check on the patient and the quality of the respiratory signal (adjust the respiratory belt if required).

NOTE: Adjustment of the belt should only be performed when no respiratory gated bed positions are acquired. Therefore, adjustments should be done before or after these bed positions are acquired. Adjustment of the belt during acquisition of the gated bed position will affect the quality of the ORG images. Careful observation of the respiratory signal and possible adjustment of the respiratory belt before acquisition of the gated bed positions is required to counteract any significant baseline drifting of the signal during PET scanning.

2.2. Image reconstruction

2.2.1. Review the respiratory signal that has been acquired and select the appropriate duty cycle for the gated bed positions.

NOTE: The amplitude range used for respiratory gating is superimposed on the respiratory signal). Check for inconstancies or baseline drifts in the respiratory signal that can influence quality of the respiratory gating.

2.2.2. Select image reconstruction protocol optimized for viewing (**Figure 7**). This is usually a high-resolution image reconstruction protocol with smaller voxel sizes for detection of small lesions. It is of importance to realize that the ORG algorithm will calculate the optimal amplitude range by using the entire respiratory signal of the selected bed positions. Though different duty

cycles can be used for different bed positions (for example to correct for a varying quality respiratory signal), using different duty cycles for different bed positions is not advised given that this will introduce variations in image quality between different bed positions.

NOTE: Here is an example image reconstruction protocol for viewing:

- Algorithm: TrueX + TOF (UltraHD PET)
- Number of iterations: 3
- Number of subsets: 21
- Matrix size: 400 × 400
- Post-reconstruction filtering, kernel (3D Gaussian), full width half maximum (FWHM): 3.0 mm
- Duty cycle 35%

2.2.3. Furthermore, reconstruct the PET images with an protocol compliant to the Research4Life (EARL) initiative for quantitative PET imaging. These are usually lower resolution images with specific post-reconstruction filtering applied.

NOTE: Here is an example image reconstruction protocol for image quantification:

- Algorithm: TrueX + TOF (UltraHD PET)
- Number of iterations: 3
- Number of subsets: 21
- Matrix size: 256
- Post-reconstruction filtering, kernel (3D Gaussian), full width half maximum (FWHM): 8.0 mm
- Duty cycle 35%

2.2.4. Send the reconstructed images to the PACS archive. The images are now ready to be evaluated by the nuclear medicine physician

REPRESENTATIVE RESULTS:

The use of ORG in PET images results in an overall reduction of respiratory-induced blurring of the images. For example, in a clinical evaluation of patients with non-small cell lung cancer (NSCLC), ORG resulted in detection of more pulmonary lesions and hilar/mediastinal lymph nodes²⁰. This is readily demonstrated in **Figure 8** and **Figure 9**, showing non-gated and ORG PET images of patients with NSCLC.

In particular, ORG resulted in management changes in patients with early disease stages (I-IIb) where detection of additional lesions of lymph nodes can significantly affect the prescribed treatment and additional diagnostic procedures required. These results are confirmed by a study conducted by van der Gucht et al. for lesions located in the upper abdomen²¹. The use of ORG resulted in detection of more lesions in FDG-PET of patients with hepatic and perihepatically located lesions. Although these results support that the use of ORG may lead to improved diagnosis and staging of patients, the exact clinical impact of ORG remains unclear.

Image quantification is significantly impacted when ORG was used to correct PET images for respiratory motion, particularly for pulmonary lesions located near the diaphragm and hilar regions of the lungs. In a study investigating the effects of ORG in 66 lung cancer patients, there was a statistically significant increase in mean SUV (SUV_{mean}) uptake in the ORG images with respect to the non-gated PET images. Compared to the non-gated PET images, the ORG PET images showed an increase in SUV_{mean} of $6.2 \pm 12.2\%$ ($p < 0.0001$), $7.4 \pm 13.3\%$ ($p < 0.0001$), and $9.2 \pm 14.0\%$ ($p < 0.0001$), for duty cycles of 50%, 35% and 20% respectively¹².

Furthermore, a statistically significant decrease in metabolic volumes of the lesions was observed when ORG was performed. These volumes were segmented using a region growing fixed threshold (40% of the maximum uptake (SUV_{max})) segmentation algorithm. There was a decrease of $6.9 \pm 19.6\%$ ($p = 0.02$), $8.5 \pm 19.3\%$ ($p < 0.0001$), and $11.3 \pm 20.2\%$ ($p < 0.0001$) for duty cycles of 50%, 35%, and 20% respectively¹². The significant increase in uptake and decrease in metabolic volume indicate effective removal of respiration-induced image blurring from the PET images when ORG is performed. Additionally, it was shown that the influence of respiratory motion artefacts on quantification of lesion uptake and volume was dependent on anatomical location. There was only a significant increase in SUV_{mean} and decrease in volume for lesions located in the lower lung lobes and centrally (particularly hilar) located lesions. The effect of anatomical location is readily demonstrated in Figure 10, showing two different NSCLC lesions in a single patient. Furthermore, comparing the ORG PET images reconstructed images with a duty cycle of 35% to their non-gated equivalent images showed that the levels of image noise are comparable, demonstrating that image quality is kept constant when using ORG¹².

The relation between duty cycle and image noise was demonstrated by calculating the coefficient of variation (COV) of FDG uptake in unaffected lung parenchyma. The COV in non-gated images using all data available was on average $26.1 \pm 6.4\%$, whereas the COV in ORG PET images reconstructed with a duty cycle of 20% was $39.4 \pm 7.5\%$. There was a non-significant difference in COV between ORG PET images reconstructed with a duty cycle of 35% ($32.8 \pm 6.4\%$) and their non-gated equivalent images ($31.8 \pm 5.6\%$). **Figure 11** shows two different ORG PET and non-gated PET images with different statistical quality. This figure demonstrates that lowering the duty cycle increases the amount of noise, while the statistical quality of the ORG PET image reconstructed with a duty cycle of 35% and the non-gated equivalent image is kept constant. Although ORG results in significant reduction of lesion volume as quantified on PET images, the absolute reduction in volume yielded no significant sparing of the radiation dose delivered to the organs at risk (OARs) during radiotherapy planning, as demonstrated in another study²².

The blurring effect of respiratory motion is also affecting quantification of intra-tumor heterogeneity. In a cohort of 60 NSCLC patients, ORG demonstrated statistically significant differences in texture feature quantification of lesions in the middle and lower lung lobes²³. For the textural features; high-intensity emphasis (HIE), entropy, zone percentage (ZP), and dissimilarity, the relative increase was $16.8\% \pm 17.2\%$ ($p = 0.006$), $1.3\% \pm 1.5\%$ ($p = 0.02$), $2.3\% \pm 2.2\%$ ($p = 0.002$), $11.6\% \pm 11.8\%$ ($p = 0.006$) between the ORG PET images and their non-gated equivalent PET images. Quantification of global intra-tumor heterogeneity was not significantly

affected for lesions in the upper lung lobes. The mean decrease of these textural features was of $1.0\% \pm 7.7\%$ ($p = 0.3$), $0.35\% \pm 1.8\%$ ($p = 0.3$), $1.7\% \pm 13.2\%$ ($p = 0.4$), and $0.4\% \pm 2.7\%$ ($p = 0.5$), for dissimilarity, entropy, HIE, and ZP respectively. Furthermore, there was no significant difference in between ORG and non-gated PET images for centrally located lesions, with a mean increase of $0.58\% \pm 3.7\%$ ($P = 0.6$), $5.0\% \pm 19.0\%$ ($P = 0.4$), $0.59\% \pm 4.0\%$ ($P = 0.9$), and $4.4\% \pm 27.8\%$ ($P = 0.4$), for entropy, dissimilarity, ZP, and HIE respectively. Although quantification of textural features was significantly affected for lesions located in the middle and lower lung lobes, the multivariate Cox regression models for survival were not significantly affected²³. In addition to quantification of intra-tumor heterogeneity of pulmonary lesions, respiratory motion can result in significant changes in quantification of intra-tumor heterogeneity of lesions located in the upper abdominal region. This is readily demonstrated in a study investigating the effect of ORG on the quantification of patients with a pancreatic ductal adenocarcinoma (PDAC)²⁴. Removal of respiratory motion artifacts from PET images using ORG considerably affects quantification of textural features in PDAC lesions. It was observed that the correlation of the calculated texture features with overall survival was significantly affected.

FIGURE AND TABLE LEGENDS:

Figure 1. a) Physiological distribution of ^{18}F -fluorodeoxyglycose (FDG) in a patient who underwent positron emission tomography (PET) imaging. There is significant uptake of FDG in the heart, brain, and liver of the patient. b) Increased FDG-uptake in multiple lung, lymph node and distant metastases in a patient with stage IV non-small cell lung cancer (NSCLC), demonstrating the preferential uptake of FDG in cancer lesions when compared to most other non-affected tissues.

Figure 2. Phase- and amplitude-based gating in positron emission tomography (PET). a) Phase-based gating, b) amplitude-based gating, and c) optimal respiratory gating (ORG). During phase-based gating, each respiratory cycle is subdivided into a fixed number of gates (in this case 4). Data collected in a specific gate will be used to reconstruct an image from which the main respiratory motion components will be removed. Amplitude-based gating relies on definition of an upper and lower amplitude limit. Amplitude-based respiratory gating approaches typically rely on specification of an amplitude-range by the user. Data collected when the respiratory signals falls within the defined amplitude range will be used for image reconstruction. The optimal respiratory gating (ORG) algorithm uses such an amplitude-based approach and will calculate an optimal amplitude range based on the duty cycle (percentage of the PET data that is required for image reconstruction) provided. The smallest amplitude range that still contains the specified amount of data that is required for image reconstruction (total sum of the areas shaded in blue) is selected as the optimal amplitude range (W). In order to achieve this, the ORG algorithm adjusts the upper limit (U) for different values of the lower limit (L). Generally, increasing the number of gates or reduction of the amplitude range will result in a more effective rejection of respiratory motion at the cost of increased image noise.

Figure 3. Selection of appropriate imaging protocol. A predefined imaging protocol can be selected by selecting a protocol from a specific category (by hovering the mouse over the protocol categories (indicated by the red box) and select a protocol from the drop-down menu).

Figure 4. Different keys on the control box of the Siemens mCT and Horizon PET/CT scanners.

1) Move Key, used to move the patient table to the next measuring position, 2) Unload patient key: used to move the patient table to the unload position after image acquisition, 3) Start key: Used to trigger a scan, the radiation warning sign (4) will light up during image acquisition, 4) Radiation warning lamp: Indicates and provides a warning signal when X-ray tube is on, 5) Suspend key: Used to hold the scan procedure. This is the preferred method for interrupting a scan before completion. The suspend option permits restart of the image protocol at the point it was halted, 6) Hear patient key: Press this key to hear the patient, the light diode indicates that the listening connection is active, press this key again to release the listening connection, 7) Loudspeaker, 8) Call patient key: Hold down this key while speaking to the microphone (10) to provide instructions to the patient, 9) Stop key: Used to immediately stop the scanning procedure, used in case of an emergency, 10) Microphone.

Figure 5. After acquisition of the topogram, the acquisition time of different bed positions have to be specified (in the 'Routine' tab). In this example, the gated bed positions are recorded for 6 minutes (bed 2), while the non-gated bed positions are acquired in 2 minutes (bed 1 and 3). Gated bed positions (highlighted in orange in the topogram) can be set by setting the option 'Physio' to 'On' in the second column.

Figure 6. Respiratory waveform of the patient is displayed in the upper part of the dashboard together with a histogram of the breathing frequency (lower part) in the 'Trigger' tab. The duty cycle can be selected from the drop-down menu on the right (in this case 35%). This protocol has a standard image acquisition time of 6 minutes per bed position for gated bed positions and 2 minutes for non-gated bed positions.

Figure 7. Selection of image reconstruction protocol ('Recon' tab), details of image reconstruction can be specified for each protocol by filling in the relevant fields. For viewing, a high resolution image reconstruction protocol is advised to provide detail in the reconstructed PET images. For quantification of radiotracer uptake on PET images, the use of an EARL compliant reconstruction protocol is advised.

Figure 8. Non-gated and optimal gated (ORG) FDG-PET-CT images of a patient with non-small cell lung cancer (NSCLC). This figure shows non-gated (a) and ORG PET (b) images of a hilar lymph node in station X in a patient with a solitary NSCLC lesion in the left lower lobe. The ORG PET image is reconstructed with a 35% duty cycle. Reduction of the blurring effects of respiratory motion would have resulted in upstaging of this patient from cT1N0M0 to cT1N1M0 and the requirement for histological evaluation of the hilar lymph node using endobronchial ultrasound (EBUS). This figure has been modified from Grootjans *et al.* (Lung Cancer 2015).

Figure 9. Non-gated (a) and optimal respiratory gated (ORG) (b) FDG-PET-CT image of a primary NSCLC lesion and satellite lesion in the right lung hilum. The primary lesion is indicated by a 'p' while the satellite lesion is indicated by a 's' in this figure. Respiratory gating in this patient resulted in improved contrast recovery of satellite lesions adjacent to the primary lesion. The

presence of the lesion was confirmed on follow-up CT imaging, although these findings would not have significantly impacted clinical management for this patient, ORG resulted in detection of additionally pulmonary lesions. This figure has been modified from Grootjans *et al.* (Lung Cancer 2015).

Figure 10. Non-gated and optimal respiratory gated (ORG) FDG-PET–CT images of a patient with NSCLC lesions in the left lower lobe and lung hilum. This example shows the effect of respiration-induced motion blurring on visualization and quantification of NSCLC lesions. **a)** Non-gated PET image depicting a lesion in the left lower lobe, **b)** ORG PET image, reconstructed with a duty cycle of 35% of a lesion in the left lower lobe, **c)** Non-gated PET image depicting a lesion in the left lung hilum, **d)** ORG PET image, reconstructed with a duty cycle of 35% of a lesion in the left lung hilum. In this patient, the lesion located in the lung hilum is subjected to considerable respiration-induced motion, showing a large effect on quantification of lesion uptake and metabolic volume when ORG is performed. For this lesion, an increase in mean standardized uptake value (SUVmean) of 31.9% and decrease in metabolic volume of 23.0% was observed. The effect of respiratory motion on quantification of lesion uptake and volume was 5.3% and 1.9% respectively for the lesion in the upper lung lobe. This figure has been modified from Grootjans *et al.* (Eur Radiol 2014).

Figure 11. Comparison of optimally respiratory gated (ORG) and non-gated PET images with different counts statistics in a patient with stage IV non-small cell lung cancer (NSCLC). The left column (**a** and **c**) display the non-gated PET images reconstructed with all (**a**) and 35% (**c**) of the recorded data. Comparing images **a** and **c** reveals that noise levels are increased when less data is used for image reconstruction, particularly noticeable in the areas of relatively homogeneous uptake, such as the liver (indicated with an asterisk '*'). The column on the right (**b** and **d**) displays the ORG PET images reconstructed with 50% and 35% duty cycle. These images show that the amount of noise is increased when the duty cycle is lowered. Comparing the non-gated PET image (**c**) with its ORG PET equivalent (**d**) shows that the respiratory-induced blurring effect is reduced in the ORG image, which is reflected by the apparent size of the metastatic lesion in the adrenal gland (indicated with a plus sign '+') and renal calices of the left kidney (indicated with an 'x').

DISCUSSION:

In the nuclear medicine community, the deteriorating effects of respiratory motion artefacts in PET imaging have been well-recognized for a long time. It has been shown in many studies that the blurring effect of respiratory motion artefacts can significantly influence image quantification and lesion detectability. Although several respiratory gating methods have been developed, respiratory gating is currently not widely being used in clinical practice. This is particularly due to a resulting variable image quality, unacceptable prolongation of image acquisition times, non-ideal integration of respiratory gating in a clinical full body imaging protocol. The advantage of ORG is that it permits convenient integration in a standard whole-body PET imaging protocol, making it possible to seamlessly integrate multiple gated and non-gated bed positions in a single image. Furthermore, the ORG algorithm takes specific characteristics of the entire respiratory signal, such as plateau phases, into account when calculating the optimal amplitude range, while the user has the ability to directly specify the image quality of the reconstructed PET images by

specifying the duty cycle. However, similar to many other respiratory gating methods, ORG requires the use of external sensors which is used to perform respiratory gating. Furthermore, depending on the duty cycle used, a considerable amount of PET data is discarded and not used for reconstruction of the final image. Therefore, successful respiratory gating with ORG relies on appropriate tracking of respiratory motion using external sensors and lengthening image acquisition times or the amount of administered activity to the patients. The difficulty related to the use of sensors inspired the development of data-driven, or sensor-less respiratory gating approaches^{25,26,27}. These data-driven techniques omit the requirement for an external surrogate signal by extracting information on respiratory motion from the PET list-mode data itself. Such data-driven techniques have been developed by multiple PET vendors and have been proposed as clinically applicable alternatives to sensor-based methods, facilitating routine PET respiratory gating in clinical practice.

In addition to solely extracting information regarding respiratory motion from PET data, newer methods permit the use of all PET data being recorded for image reconstruction²⁸. These motion-compensated image reconstructions are performed by elastically transforming PET data from different respiratory phases to a single image from which motion artefacts are removed. Compared to traditional sensor-based respiratory gating, motion-compensated reconstruction does not require lengthening of image acquisition time and prevent the use of additional hardware during gating. These methods effectively remove respiratory motion from PET images whilst maintaining image quality²⁹. Furthermore, with the emergence of hybrid PET and magnetic resonance (MR) imaging, several methods have been developed that use motion information derived from MR to correct PET images^{30,31,32,33}. Though these methods have existed for some time in a research setting, the first data-driven respiratory gating methods have entered the market. However, most of these methods are still under active development and continuous improvement and larger clinical studies are required to evaluate the performance and robustness of such algorithms.

Although respiratory gating methods are mainly focused on correcting PET images for respiratory motion artefacts, these algorithms usually do not take the acquired CT data into consideration. In clinical practice, low-dose (LD) CT is usually performed without providing breathing instructions. Registration of a LDCT acquired when the patient is breathing freely can result in a significant spatial mismatch between respiratory gated PET and LDCT, particularly for anatomical structures that move during respiration³⁴. In addition to accurately localize radiotracer uptake, the LDCT is used for attenuation correction of the PET images. Therefore, the effect of a spatial mismatching between PET and CT can introduce profound quantitative inaccuracies in PET, particularly when radiotracer uptake is located near structures with large differences in density, such as lung and bone tissue. Several authors have investigated different methods to synchronize image acquisition to reduce spatial mismatching between PET and CT images. One proposed method involves providing breathing instructions to the patient during CT acquisition. Although standard CT breathing instructions in combination with ORG did not yield an improvement in spatial matching between CT and PET³⁵, patient-specific instructions based on the same respiratory signal and amplitude range used for ORG did result in an overall improvement of the spatial match between PET and CT³⁶. However, these methods are sensitive to variations in

operator instructions and patient interpretation. Improved results have been obtained by performing training sessions with the patient before PET-CT imaging. However, given that some patients have difficulty complying to these breathing instructions due an impaired physical condition, success might remain variable in a clinical setting. Other approaches include the use of respiratory triggered CT, where the respiratory signal is used to trigger the CT acquisition³⁴. This approach in combination with ORG resulted in a significant reduction in spatial mismatch between PET and CT images. In a study evaluating a triggered to a standard CT protocol showed an increase in SUV_{max} and SUV_{mean} of 5.7% ± 11.2% (P < 0.001) and 6.1% ± 10.2% (P = 0.001), respectively. Although full 4D CT gating has been proposed to match PET and CT images, such strategies are not applicable in routine clinical practice given an unacceptably high radiation exposure to the patient. Different methods for reducing the spatial mismatch between PET and CT images are still under evaluation for their effectiveness and clinical usefulness.

Although respiratory motion significantly influences image quantification of PET images, there remain many other technical factors that have to be taken into account in order to maintain reproducibility and quantitative accuracy of PET images¹¹. These factors are related to patient preparation, imaging acquisition settings and reconstruction protocols. It is important to adhere to strict acquisition protocols, including the use of similar patient-preparation procedures, assessment of radiotracer uptake at specific time points, and scanning and reconstruction parameters^{11,37}. In this regard, the European Association of Nuclear Medicine (EANM) provides guidelines on quantitative FDG-PET-CT for multicenter comparisons. It has been shown that harmonization of imaging protocols using standardized guidelines results in overall improved comparability of PET images from different institutions³⁸.

ACKNOWLEDGMENTS:

The authors would like to thank Richard Raghuo for providing the PET images shown in **Figure 1**.

DISCLOSURES:

The authors declare no conflict of interest.

REFERENCES:

1. Kostakoglu, L., Agress, H., Goldsmith, S.J. Clinical Role of FDG PET in Evaluation of Cancer Patients. *Radiographics*. **23** (2), 315-340 (2003).
2. Grootjans, W. et al. PET in the management of locally advanced and metastatic NSCLC. *Nature Reviews Clinical Oncology*. **12** (7), 395-407 (2015).
3. Croteau, E. et al. PET Metabolic Biomarkers for Cancer. *Biomarkers in Cancer*. **8** (Suppl 2), 61-69 (2016).
4. Vlenterie, M. et al. Early Metabolic Response as a Predictor of Treatment Outcome in Patients With Metastatic Soft Tissue Sarcomas. *Anticancer Research*. **39** (3), 1309-1316 (2019).
5. Barrington, S.F., Meignan, M.A. Time to prepare for risk adaptation in lymphoma by standardising measurement of metabolic tumour burden. *Journal of Nuclear Medicine*. **60** (8), 1096-1102 (2019).
6. Grootjans, W. et al. Performance of automatic image segmentation algorithms for calculating total lesion glycolysis for early response monitoring in non-small cell lung cancer

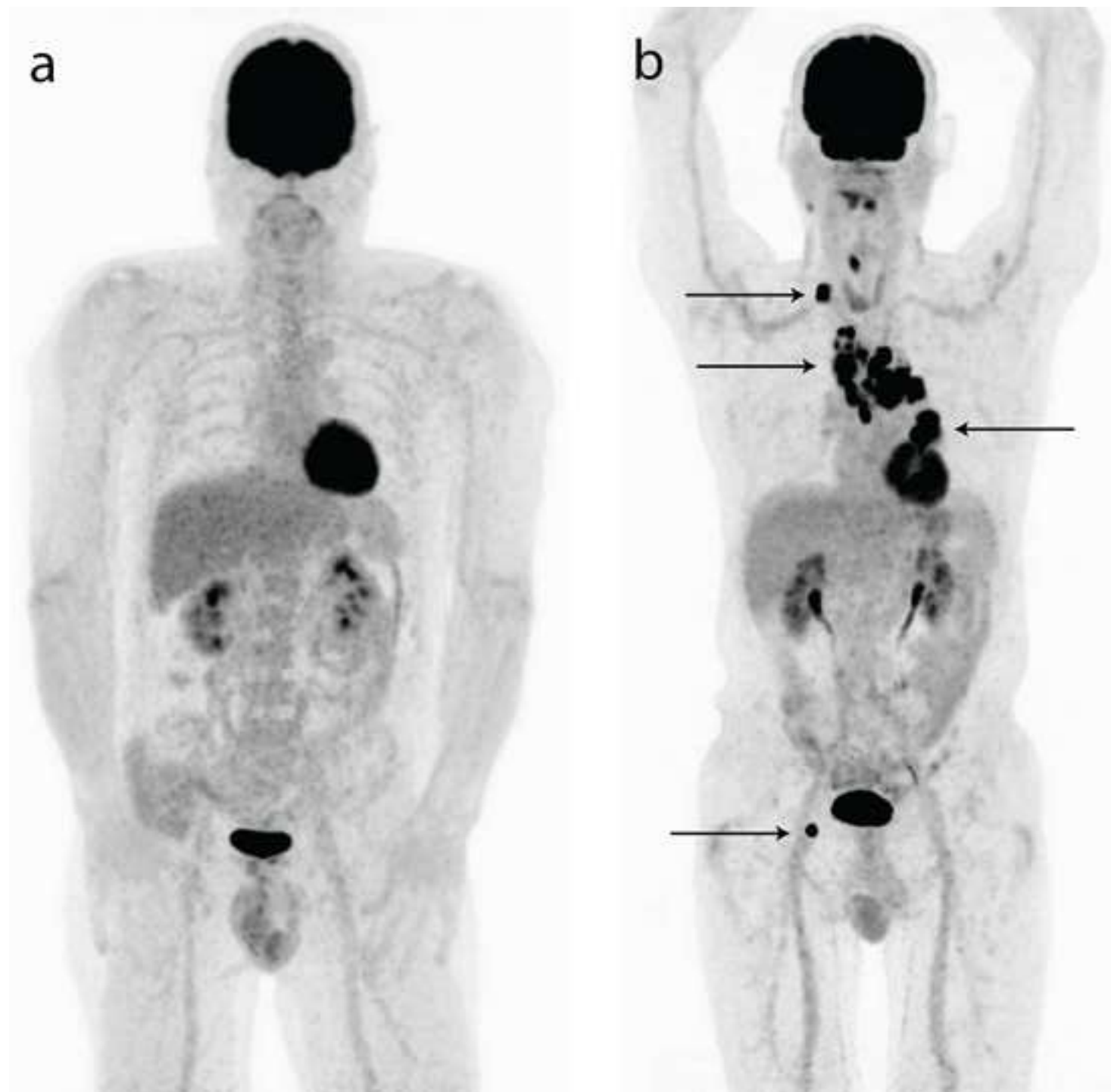
- patients during concomitant chemoradiotherapy. *Radiotherapy and Oncology*. **119** (3), 473-479 (2016).
7. Grootjans, W., Geus-Oei, L.F., Bussink, J. Image-guided adaptive radiotherapy in patients with locally advanced non-small cell lung cancer: the art of PET. *Quarterly Journal of Nuclear Medicine and Molecular Imaging*. **62** (4), 369-384 (2018).
8. Everitt, S. et al. Acute radiation oesophagitis associated with 2-deoxy-2-[18F]fluoro-d-glucose uptake on positron emission tomography/CT during chemo-radiation therapy in patients with non-small-cell lung cancer. *Journal of Medical Imaging and Radiation Oncology*. **61** (5), 682-688 (2017).
9. Castillo, R. et al. Pre-radiotherapy FDG PET predicts radiation pneumonitis in lung cancer. *Radiation Oncology*. **74** (9), 1-10 (2014).
10. Lee, J.W., Seo, K.H., Kim, E.S., Lee, S.M. The role of 18F-fluorodeoxyglucose uptake of bone marrow on PET/CT in predicting clinical outcomes in non-small cell lung cancer patients treated with chemoradiotherapy. *European Radiology*. **27** (5), 1912-1921 (2017).
11. Aide, N. et al. EANM/EARL harmonization strategies in PET quantification: from daily practice to multicentre oncological studies. *European Journal of Nuclear Medicine and Molecular Imaging*. **44** (Suppl 1), 17-31 (2017).
12. Grootjans, W. et al. Amplitude-based optimal respiratory gating in positron emission tomography in patients with primary lung cancer. *European Radiology*. **24** (12), 3242-3250 (2014).
13. Dawood, M., Büther, F., Lang, N., Schober, O., Schäfers, K.P. Respiratory gating in positron emission tomography: A quantitative comparison of different gating schemes. *Medical Physics*. **34** (7), 3067-3276 (2007).
14. Fayad, H., Lamare, F., Thibaut, M., Visvikis, D. Motion correction using anatomical information in PET/CT and PET/MR hybrid imaging. *Quarterly Journal of Nuclear Medicine and Molecular Imaging*. **60** (1), 12-24 (2016).
15. Nehmeh, S.A. et al. A novel respiratory tracking system for smart-gated PET acquisition. *Medical Physics*. **38** (1), 531-58 (2011).
16. Boucher, L., Rodrigue, S., Lecomte, R., Bénard, F. Respiratory Gating for 3-Dimensional PET of the Thorax: Feasibility and Initial Results. *Journal of Nuclear Medicine*. **45** (2), 214-29 (2004).
17. Kokki, T. et al. Linear relation between spirometric volume and the motion of cardiac structures: MRI and clinical PET study. *Journal of Nuclear Cardiology*. **23** (3), 475-485 (2016).
18. van Elmpt, W. et al. Optimal gating compared to 3D and 4D PET reconstruction for characterization of lung tumours. *European Journal of Nuclear Medicine and Molecular Imaging*. **38** (5), 843-855 (2011).
19. Tsutsui, Y. et al. Accuracy of amplitude-based respiratory gating for PET/CT in irregular respirations. *Annals of Nuclear Medicine*. **28** (8), 770-79 (2014).
20. Grootjans, W. et al. The impact of respiratory gated positron emission tomography on clinical staging and management of patients with lung cancer. *Lung Cancer*. **90** (2), 217-223 (2015).
21. Van Der Gucht, A. et al. Impact of a new respiratory amplitude-based gating technique in evaluation of upper abdominal PET lesions. *European Journal of Radiology*. **83** (3), 509-515 (2014).

22. Wijsman, R. et al. Evaluating the use of optimally respiratory gated 18F-FDG-PET in target volume delineation and its influence on radiation doses to the organs at risk in non-small-cell lung cancer patients. *Nuclear Medicine Communications*. **37** (1), 66-73 (2016).
23. Grootjans, W. et al. The Impact of Optimal Respiratory Gating and Image Noise on Evaluation of Intratumor Heterogeneity on 18F-FDG PET Imaging of Lung Cancer. *Journal of Nuclear Medicine*. **57** (11), 1692-1698 (2016).
24. Smeets, E.M.M. et al. Optimal respiratory-gated [18F]FDG PET/CT significantly impacts the quantification of metabolic parameters and their correlation with overall survival in patients with pancreatic ductal adenocarcinoma. *European Journal of Nuclear Medicine and Molecular Imaging Research*. **9** (1):24, 1-10 (2019).
25. Büther, F., Vehren, T., Schäfers, K.P., Schäfers, M. Impact of Data-driven Respiratory Gating in Clinical PET. *Radiology*. **281** (1), 229-238 (2016).
26. Feng, T. et al. Self-Gating: An Adaptive Center-of-Mass Approach for Respiratory Gating in PET. *IEEE Transactions on Medical Imaging*. **37** (5), 1140-1148 (2018).
27. Schleyer, P.J., O'Doherty, M.J., Marsden, P.K., Extension of a data-driven gating technique to 3D, whole body PET studies. *Physics in Medicine & Biology*. **56** (13), 3953-3965 (2011).
28. Lamare, F., Fayad, H., Fernandez, P., Visvikis, D. Local respiratory motion correction for PET/CT imaging: Application to lung cancer. *Medical Physics*. **42** (10), 5903-5912 (2015).
29. Lamare, F. et al. List-mode-based reconstruction for respiratory motion correction in PET using non-rigid body transformations. *Physics in Medicine & Biology*. **52** (17), 5187-5204 (2007).
30. Manber, R. et al. Clinical Impact of Respiratory Motion Correction in Simultaneous PET/MR, Using a Joint PET/MR Predictive Motion Model. *Journal of Nuclear Medicine*. **59** (9), 1467-1473 (2018).
31. Rank, C.M. et al. Respiratory motion compensation for simultaneous PET/MR based on highly undersampled MR data. *Medical Physics*. **43** (12), 6234-6245 (2016).
32. Küstner, T et al. MR-based respiratory and cardiac motion correction for PET imaging. *Medical Image Analysis*. **42**, 129-144 (2017)
33. Fayad, H. et al. The use of a generalized reconstruction by inversion of coupled systems (GRICS) approach for generic respiratory motion correction in PET/MR imaging. *Physics in Medicine & Biology*. **60** (6), 2529-2546 (2015).
34. van der Vos, C.S. et al. Improving the Spatial Alignment in PET/CT Using Amplitude-Based Respiration-Gated PET and Respiration-Triggered CT. *Journal of Nuclear Medicine*. **56** (12), 1817-1822 (2015).
35. van der Vos, C.S. et al. Comparison of a Free-Breathing CT and an Expiratory Breath-Hold CT with Regard to Spatial Alignment of Amplitude-Based Respiratory-Gated PET and CT Images. *Journal of Nuclear Medicine Technology*. **42** (4), 269-273 (2014).
36. van der Vos, C.S., Meeuwis, A.P.W, Grootjans, W., de Geus-Oei, L.F., Visser, E.P. Improving the spatial alignment in PET/CT using amplitude-based respiratory-gated PET and patient-specific breathing-instructed CT. *Journal of Nuclear Medicine Technology*. **47** (2), 154-159 (2018).
37. Houdu, B. et al. Why harmonization is needed when using FDG PET/CT as a prognosticator: demonstration with EARL-compliant SUV as an independent prognostic factor in lung cancer. *European Journal of Nuclear Medicine and Molecular Imaging*. **46** (2), 421-428 (2019).

748 38. Kaalep, A. et al. EANM/EARL FDG-PET/CT accreditation - summary results from the first
749 200 accredited imaging systems. *European Journal of Nuclear Medicine and Molecular Imaging*.
750 **45** (3), 412-422 (2018).
751

Figure 1

[Click here to access/download;Figure;Figure 1\(A and B\).tif](#)



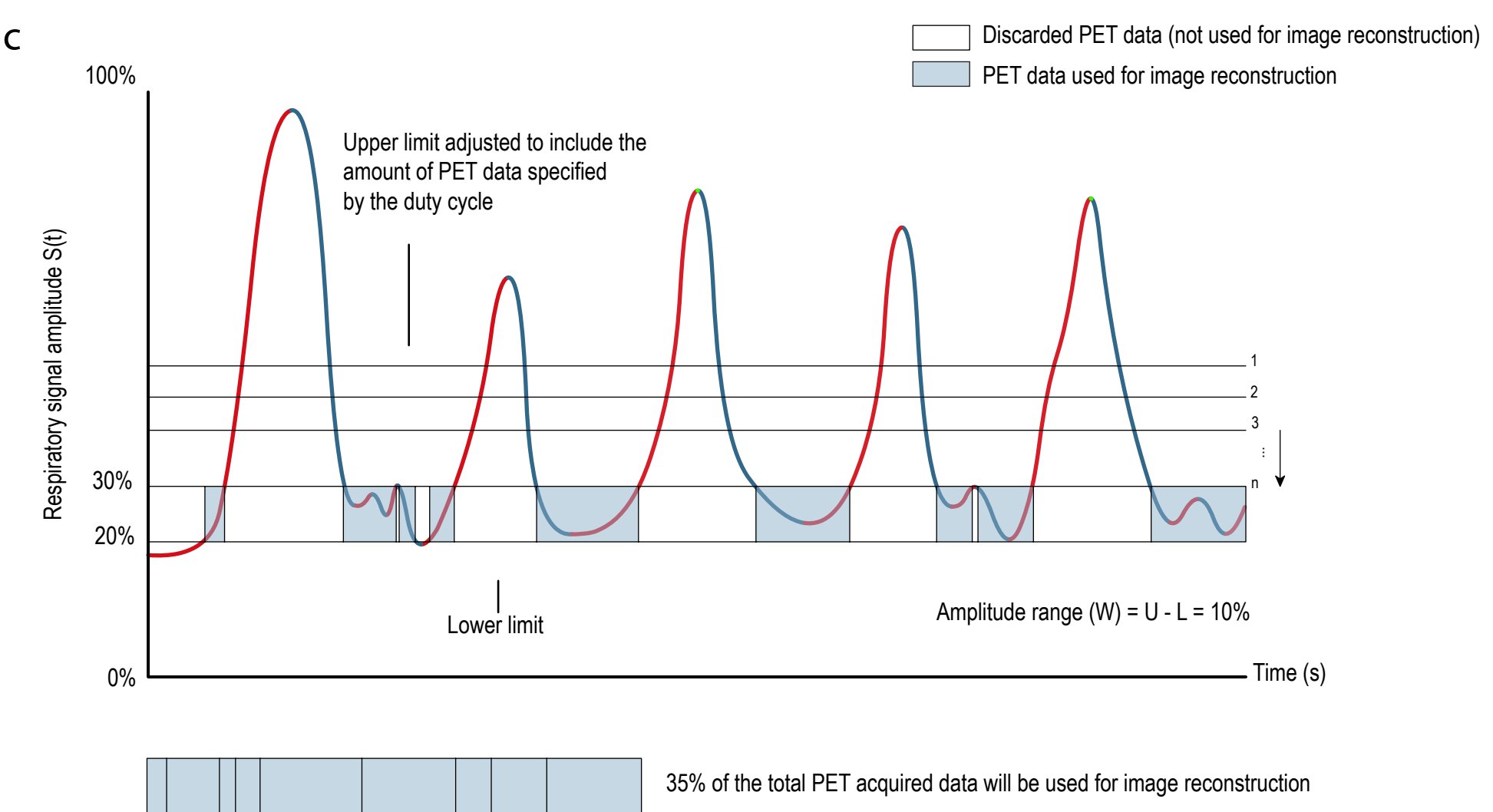
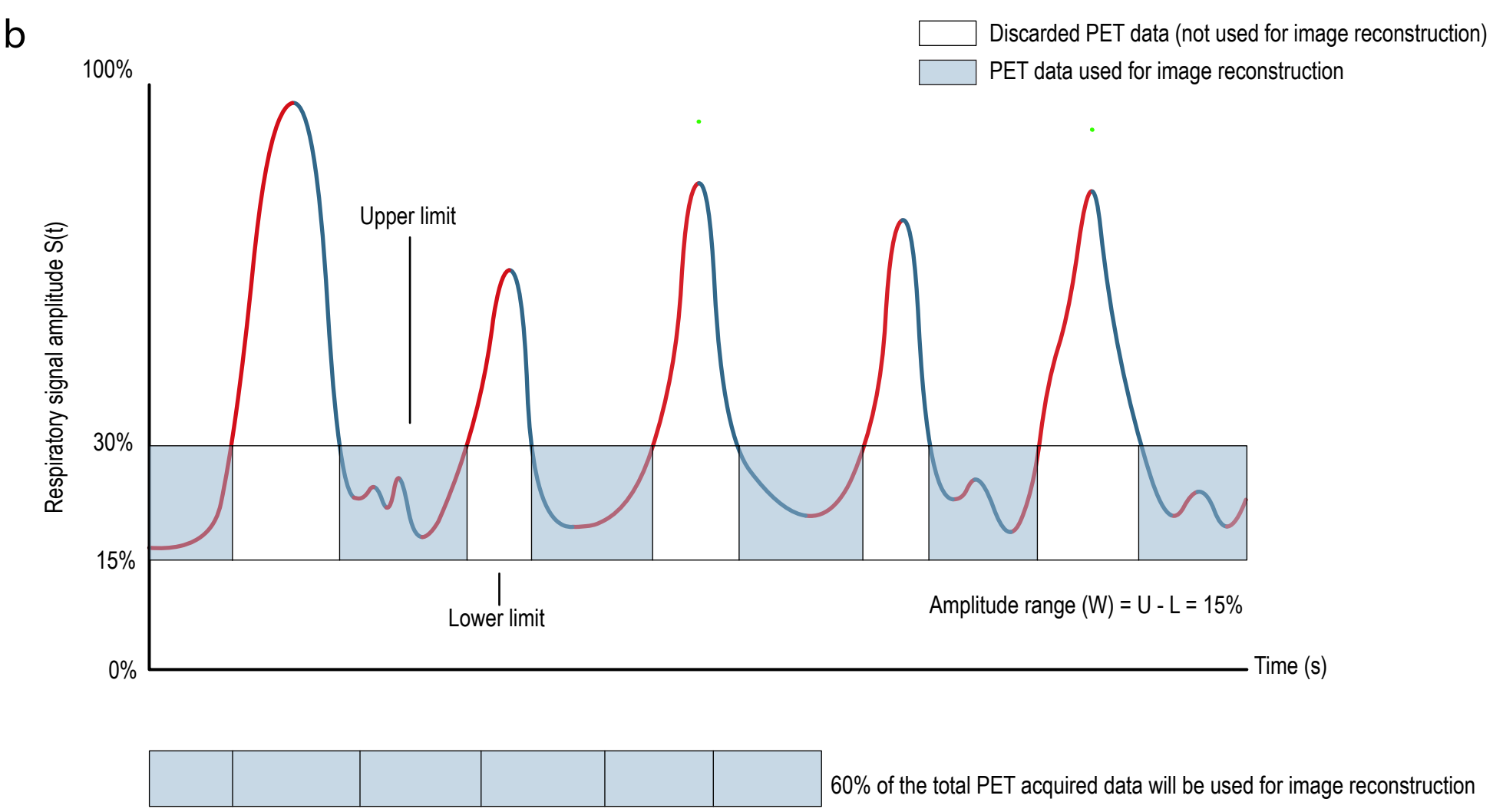
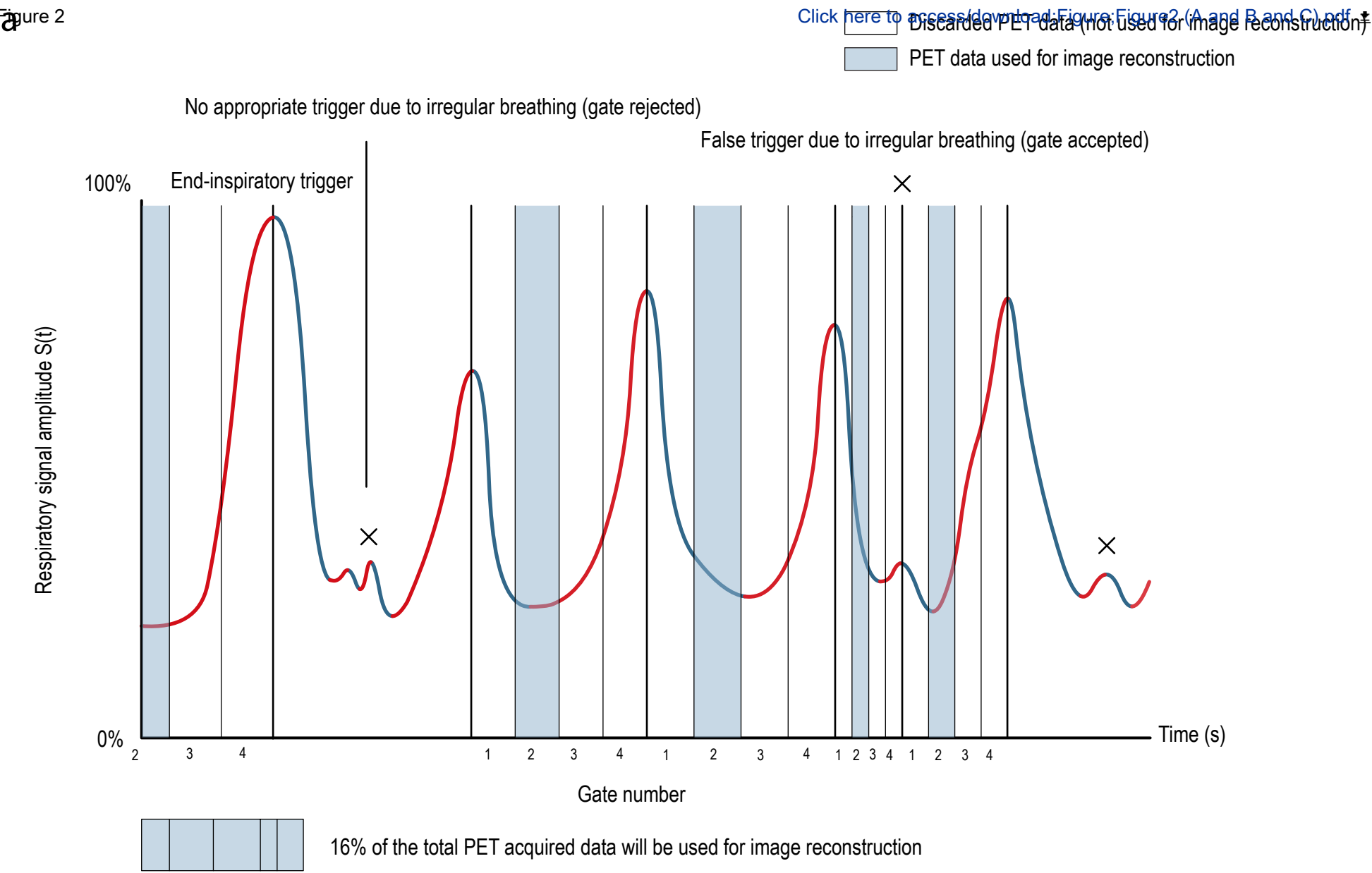


Figure 3

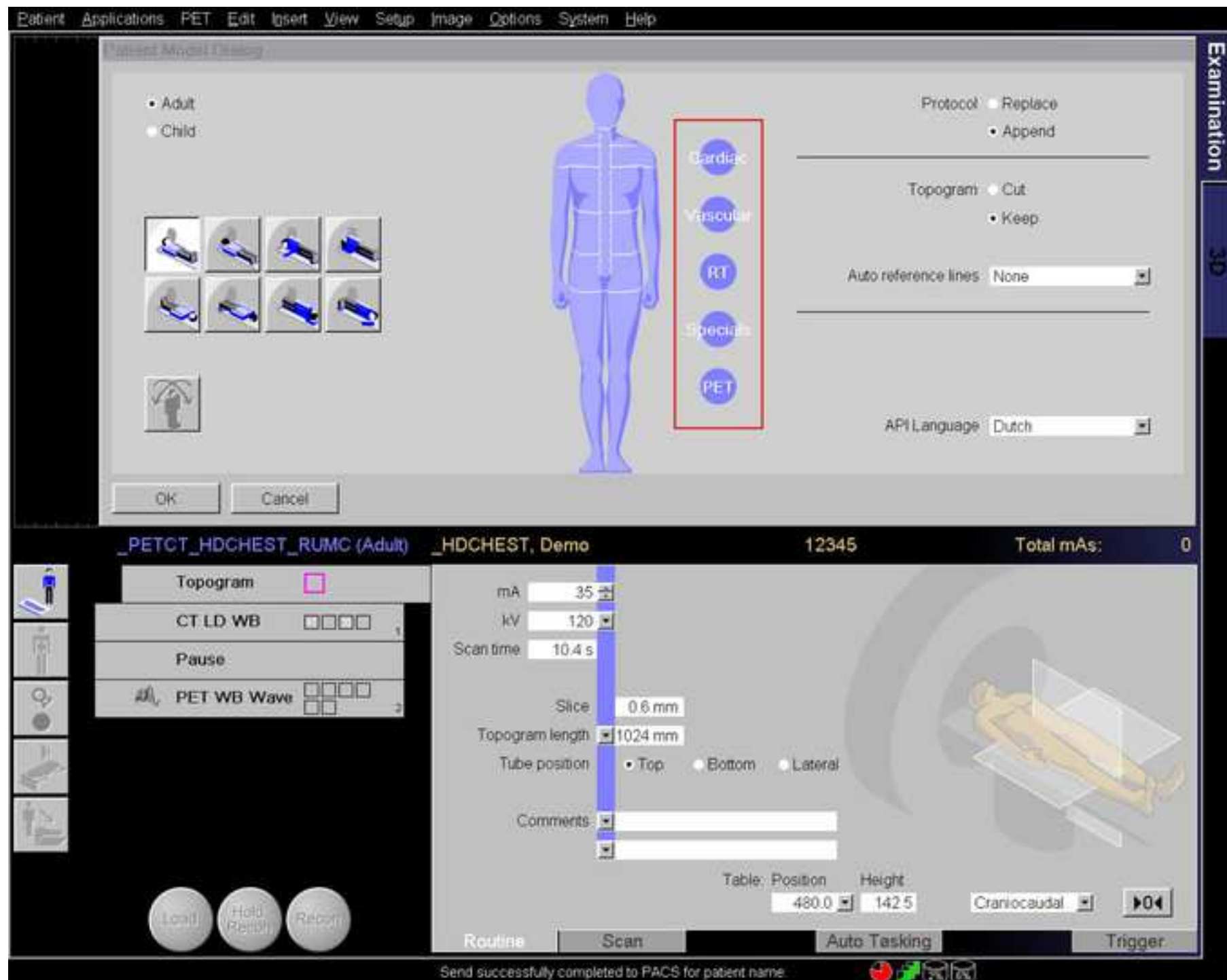


Figure 4

[Click here to access/download;Figure;Figure4.tif](#)



Figure 5

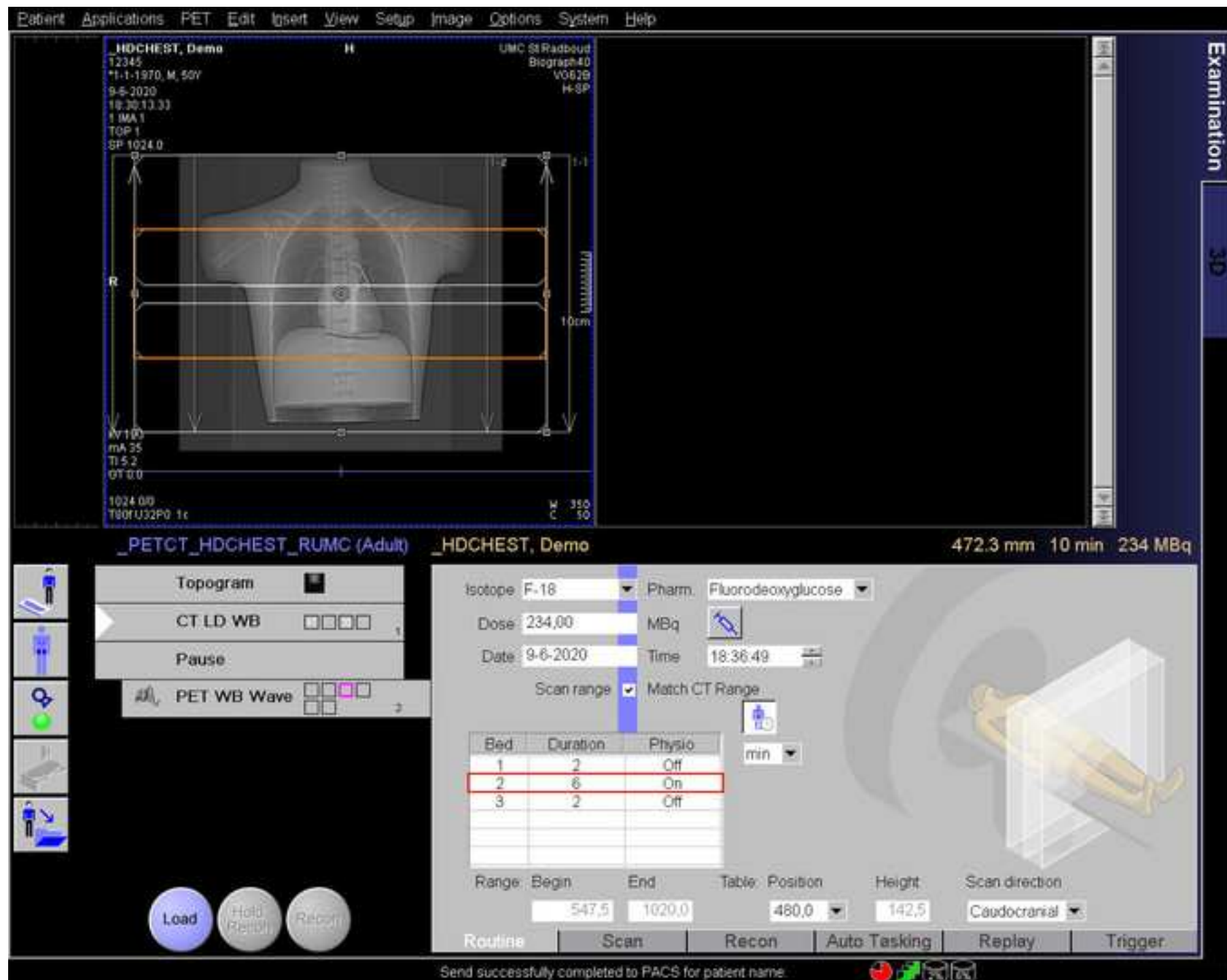
[Click here to access/download;Figure;Figure5.tif](#)

Figure 6

[Click here to access/download;Figure;Figure6.tif](#)

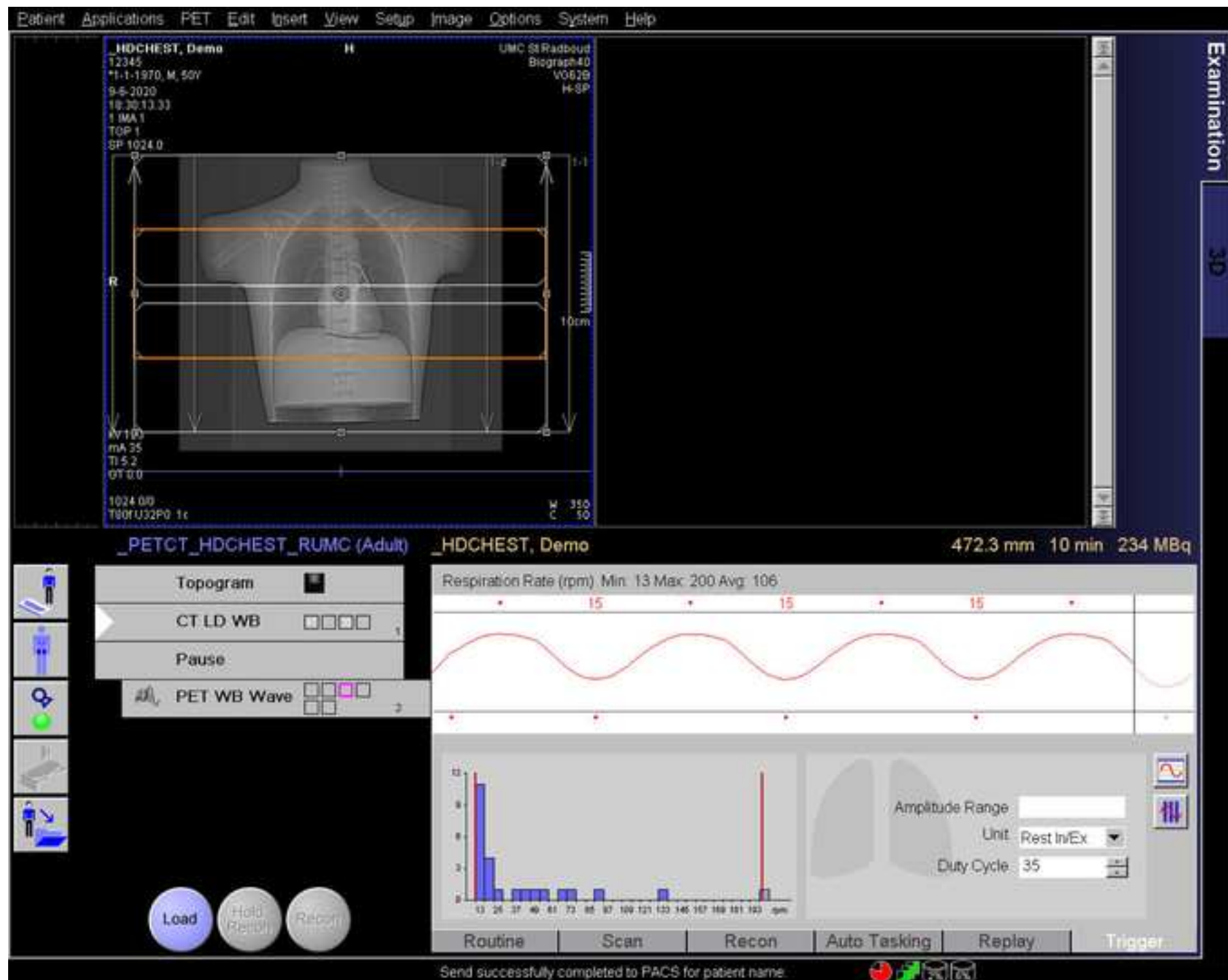
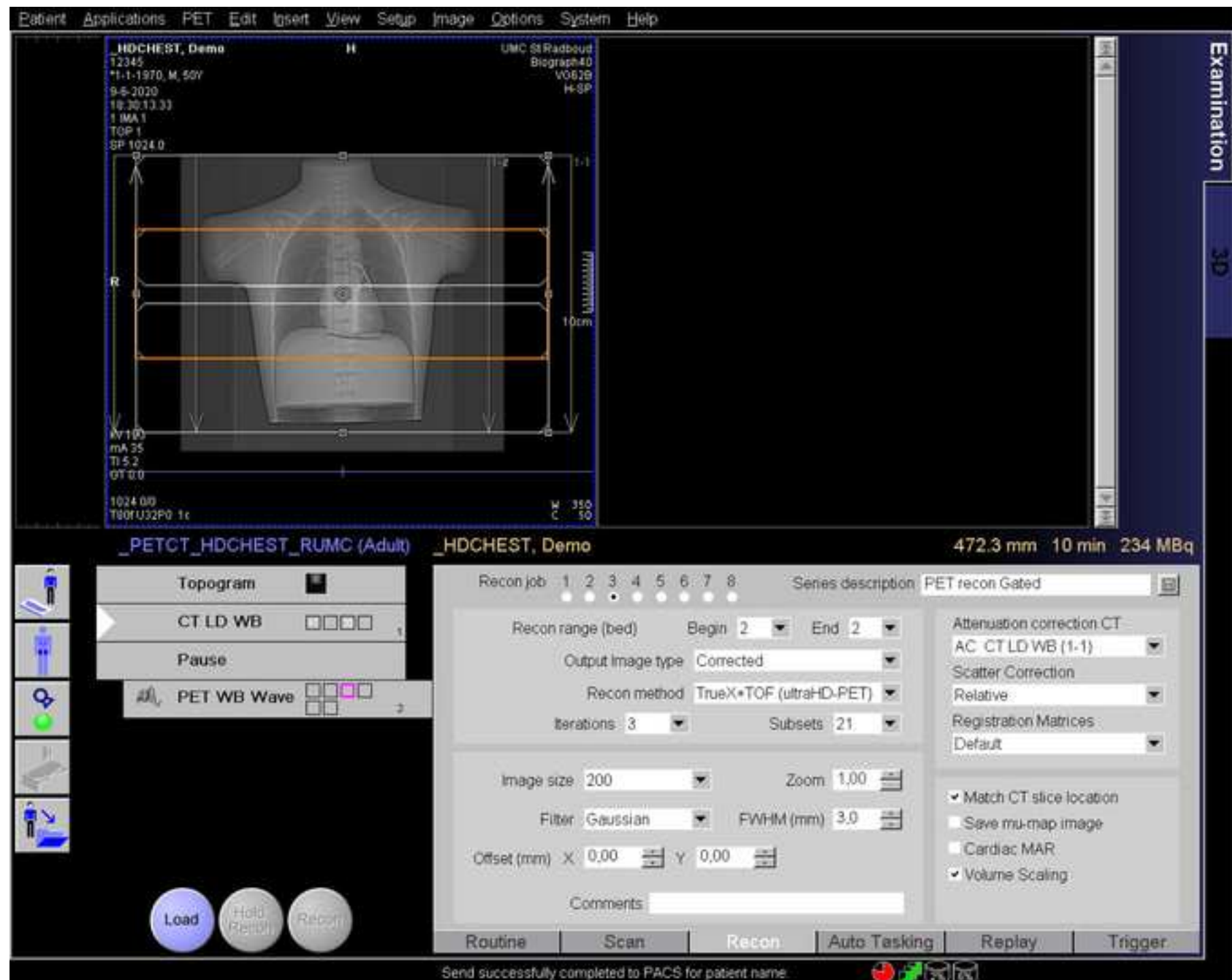
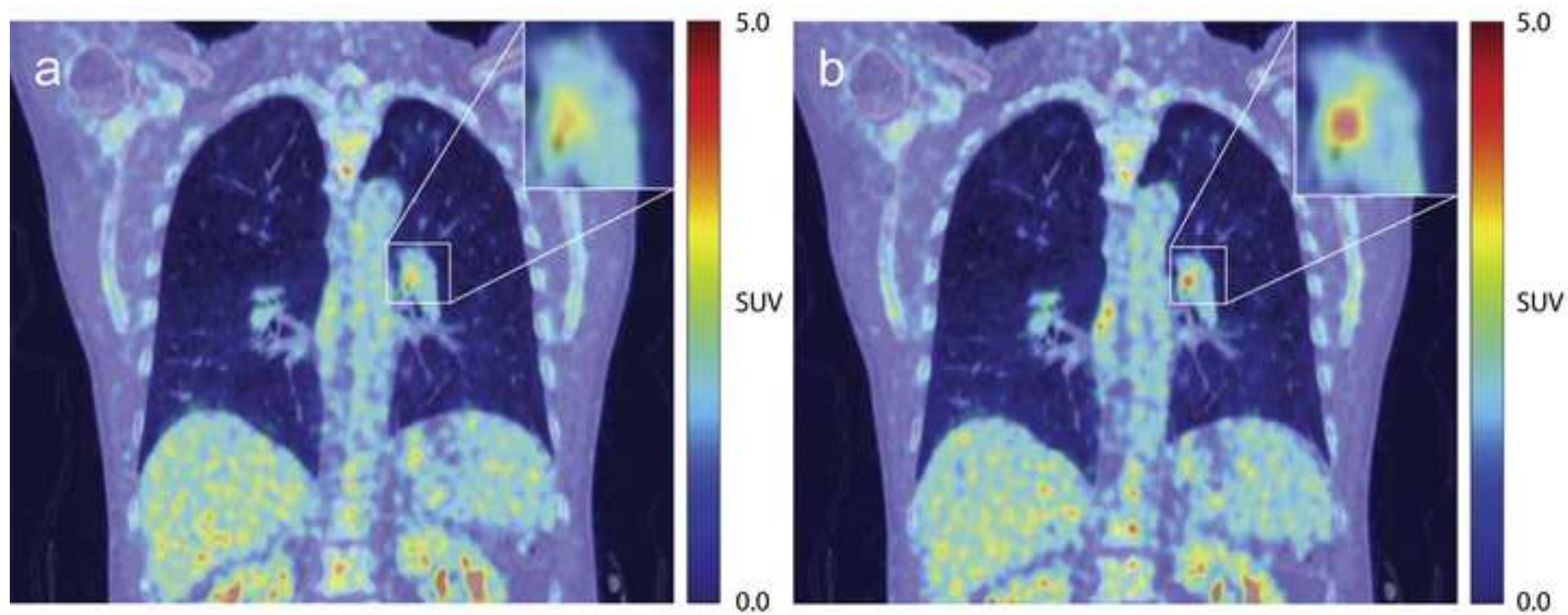


Figure 7

[Click here to access/download;Figure;Figure7.tif](#)





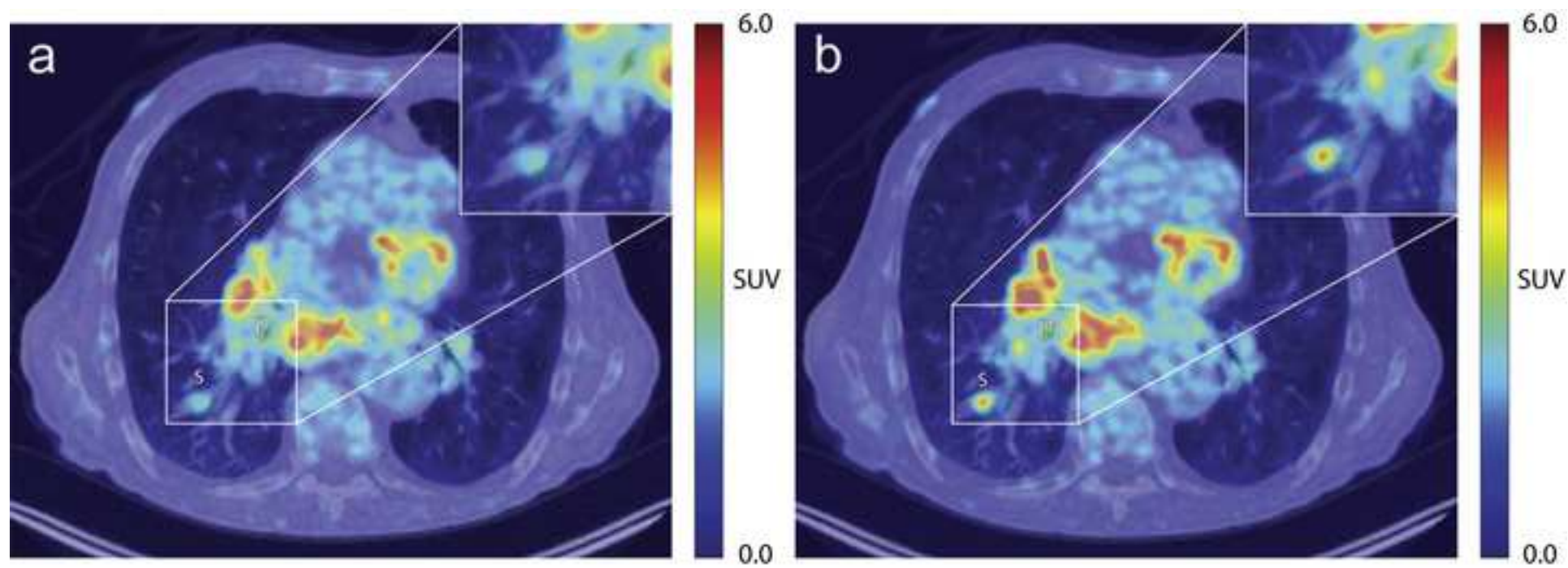


Figure 10

[Click here to access/download;Figure;Figure10 \(A, B, C, and D\).tif](#)

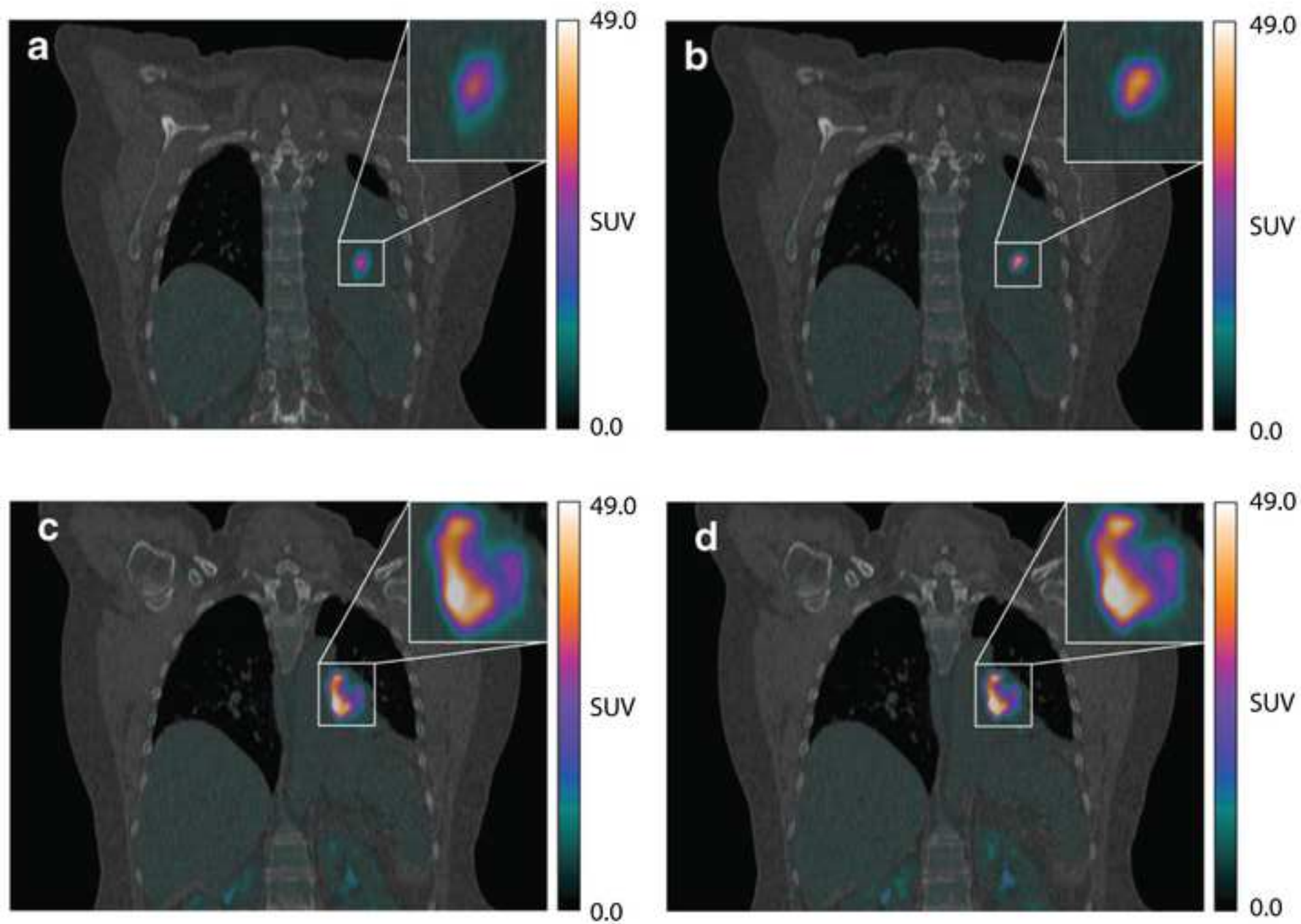
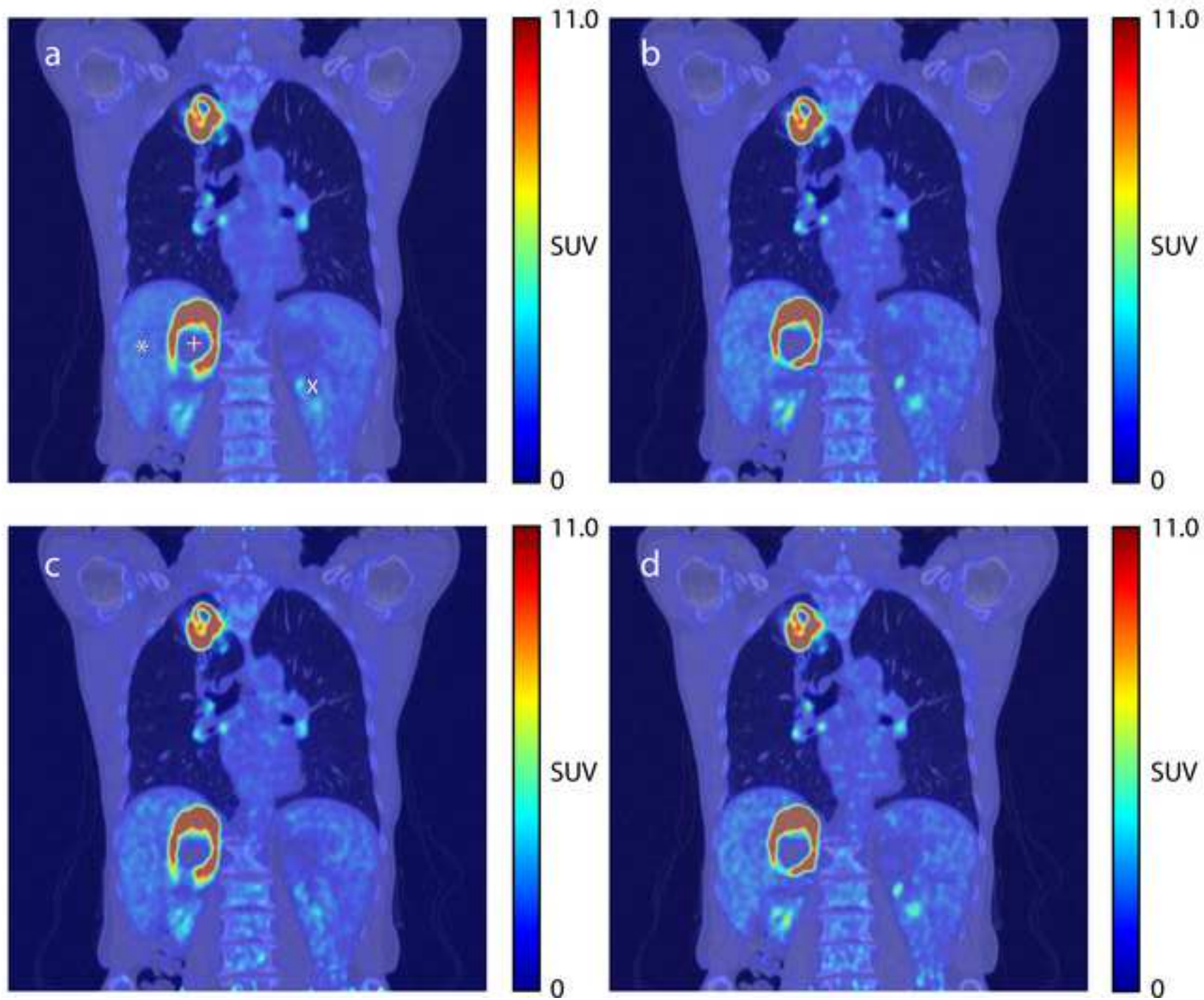
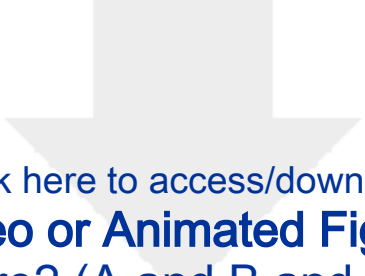


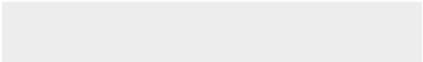

Figure 11

[Click here to access/download;Figure;Figure11 \(A, B, C, D\)-01.tif](#)





Click here to access/download
Video or Animated Figure
Figure2 (A and B and C).ai





Name of Material/ Equipment	Company
-----------------------------	---------

Sensor Port, sensor, black box, wave d anzai medical co.	
--	--

Catalog Number**Comments/Description**

respiratory gating system AZ-733V

<http://www.anzai-med.co.jp/en/product>

[/item/az733v](#)

We would like to thank the reviewers for reading the text and providing us with comments that helped us to improve the manuscript. In this point-to-point reply, we address the provided comments and suggestions.

Editorial comments:

1. Please take this opportunity to thoroughly proofread the manuscript to ensure that there are no spelling or grammar issues. The JoVE editor will not copy-edit your manuscript and any errors in the submitted revision may be present in the published version.

The manuscript has been proofread by the authors

2. Please obtain explicit copyright permission to reuse any figures from a previous publication. Explicit permission can be expressed in the form of a letter from the editor or a link to the editorial policy that allows re-prints. Please upload this information as a .doc or .docx file to your Editorial Manager account. The Figure must be cited appropriately in the Figure Legend, i.e. "This figure has been modified from [citation]."

The copy right permissions have been obtained from the publishers and a document containing the statements for re-use have been included in the submission files.

3. Please add more specific details (e.g. button clicks or menu selections for software actions, numerical values for settings, etc.) to the following steps. Please also provide specific values to be used in these steps.

4. 2.1.1: It is unclear how to select the whole-body protocol from Figure 3. Figure 3 shows "Replace" or "Append" for the protocol type.

We added a new figure where the radio-button is set on 'append' instead of 'replace', in the description of the figure, we added text to let the user know how to select a protocol.

5. 2.1.2: How to acquire a scout scan? Do you select a specific button?

The scout scan is started by pressing the round yellow button with the radiation sign. The scout scan can be stopped by either pressing the stop or abort button. We added a new figure depicting the scanner's control box with which key to press.

6. 2.1.4: Please specify the bed positions selected here. Figure 4 does not show the bed positions.

Also in line with the comments of the reviewer, we decided to create a new figure where the topogram and overlaying bed positions are visible. The description has been changed and the bed position that is gated is highlighted in an orange color

7. 2.1.6: Please specify the image recording time used. Figure 5 does not show this.

We specified the image recording time in the legend of figure 5

8. 2.2.2: Please specify the image reconstruction protocol selected.

We added further information on the two image reconstruction protocols that are selected. There are two protocols (one for viewing, which is a high resolution image) and one for image quantification (this is a lower resolution image optimized for image quantification).

9. Table of Materials: Please ensure that it has information on all relevant supplies, reagents, equipment and software used, especially those mentioned in the Protocol (e.g., radiotracer, venous cannula, syringe, etc.).

Reviewers' comments:

Reviewer #4:

I would like to thank the author for addressing all my comments thoroughly. I don't have any further comments.

We would like the reviewer for the detailed comments and suggestions provided and we are happy to hear that the changes made are to the satisfaction of the reviewer

Reviewer #7:

Manuscript Summary:

This manuscript is a good review of an optimized gating method (ORG) for PET/CT in the chest and upper abdomen. Dealing with respiratory motion is an important concept for optimal PET imaging for both visualization and quantification. This manuscript describes the set up and operation of the method that has been proposed and demonstrated elsewhere, and gives some examples of the impact of the ORG method. However, impact of this manuscript is limited as the complexity of the method is not high and the user would likely be able to implement ORG protocols with minimal guidance from either a collaborator or from the vendor depending on the setting of research or clinical deployment of ORG.

We would like to thank the reviewer for the detailed comments and suggestions, the answers to the queries are addressed below in a point-wise fashion

Minor Concerns:

Line 250: add some guidance on secondary options for the placement of the bellows.

We added some guidance on the placement of the respiratory belt around the patient (including the visual inspection and more details regarding the anatomical placement of the pressure sensor). Would this description appropriately address this point?

Line 268: should the respiratory correction beds also cover the upper abdomen as well as the thorax?

Depending on the clinical indication (whether the area of interest is located in the thoracic region or upper abdomen), the upper abdomen can be included in the gated bed positions (for example for pancreatic or liver lesions). We added this to the text.

Line 283: note that the respiratory belt should be repositioned before the acquisition of the respiratory corrected beds? Repositioning after has no impact on the acquired data.

We added some text (line 291) to explicitly say that the adjustments should be done before acquisition of the gated bed positions.

Comment on how to deal with drifting respiratory signal.

We included more text under point 2.17 on how to deal with baseline drifting. It is important to counter baseline drifting through adjustment of the belt before acquisition of gated bed positions is performed.

Comment on whether the ORG can recalculate the window, or whether the user can use different duty cycles at different points through the acquisition to optimize reconstruction if the respiratory signal quality changes.

The ORG only uses the duty cycle to calculate the optimal amplitude range. This is the only input the user can change when using ORG. Though the user can specify a different duty cycle by reconstructing different bed positions separately, this is usually not performed given that the image quality will vary per bed positions. We added a comment on this in the text (line 304 – 310).

Include a figure showing the impact of changing the duty cycle, i.e. the progression from low noise and blurry images to higher noise and sharper images, and which also shows a comparison to standard amplitude gating.

We included a figure with varying duty cycles in a single patient (figure 11). This image shows the impact of duty cycle on image noise, furthermore it shows that statistical quality of the ORG image with 35% duty cycle and its non-gated equivalent PET image is kept constant.

Part c is missing from figure 2.

We apologize for the absence of figure 2c and included this figure in the new submission of the manuscript.

For Fig 4, extend the figure to show the lower tabs that also appear on Fig 5 to show how the mode is selected.

In line with the comments of the editor we decided to create new figures. The new figure number of this figure is '5' due to insertion of another figure. The new figure displays the topogram and overlying bed positions and the whole screen (including the lower tabs).

In Fig 8, add arrows to show the extent of the primary and satellite lesions.

We included a 'p' for primary lesion and 's' for satellite lesion in the figure and updated the figure legend accordingly.

Line 471: Don't use "correct" as this method is about optimal gating not motion correction.

We change the words in this sentence.

In the comments on respiratory motion and the CT used for attenuation correction, you could introduce the ability of hybrid PET/MR to compensate and correct for motion in the AC data, the anatomical image data and the PET data.

In the discussion we put more emphasis on the hybrid PET/MR strategies for motion compensation (paragraph line 581 – 594).

Include the scanner that is used to run this ORG method. Is ORG a vendor-specific product, and is it available on other vendors?

The ORG algorithm is available only on Siemens Biograph mCT scanners and newer models. We included this information at the beginning of the protocol description (just below the ethical statement) (line 200-201).



The impact of respiratory gated positron emission tomography on clinical staging and management of patients with lung cancer

Author: Willem Grootjans, Rick Hermzen, Erik H.F.M. van der Heijden, Olga C.J. Schuurbiers-Siebers, Eric P. Visser, Wim J.G. Oyen, Loe-Fee de Geus-Oei

Publication: Lung Cancer

Publisher: Elsevier

Date: November 2015

Copyright © 2015 Elsevier Ireland Ltd. All rights reserved.

Order Completed

Thank you for your order.

This Agreement between Willem Grootjans ("You") and Elsevier ("Elsevier") consists of your license details and the terms and conditions provided by Elsevier and Copyright Clearance Center.

Your confirmation email will contain your order number for future reference.

License Number 4786991499557

[Printable Details](#)

License date Mar 13, 2020

Licensed Content

Licensed Content Publisher Elsevier
Licensed Content Publication Lung Cancer
Licensed Content Title The impact of respiratory gated positron emission tomography on clinical staging and management of patients with lung cancer
Licensed Content Author Willem Grootjans, Rick Hermzen, Erik H.F.M. van der Heijden, Olga C.J. Schuurbiers-Siebers, Eric P. Visser, Wim J.G. Oyen, Loe-Fee de Geus-Oei
Licensed Content Date Nov 1, 2015
Licensed Content Volume 90
Licensed Content Issue 2
Licensed Content Pages 7
Journal Type HS

Order Details

Type of Use reuse in a journal/magazine
Requestor type academic/educational institute
Portion figures/tables/illustrations
Number of figures/tables/illustrations 2
Format electronic
Are you the author of this Elsevier article? Yes
Will you be translating? No

About Your Work

Title of new article Management of respiratory motion artefacts in 18F-fluorodeoxyglucose positron emission tomography using an amplitude-based optimal respiratory gating algorithm
Lead author Willem Grootjans
Title of targeted journal Journal of visualized experiments
Publisher Journal of visualized experiments
Expected publication date May 2020

Additional Data

Portions Figure 2, page 220 Figure 3, page 220

Requestor Location

Requestor Location Willem Grootjans
Sigmaplasmolen 665
Leiden, 2321 KL
Netherlands
Attn: Willem Grootjans

Tax Details

Publisher Tax ID GB 494 6272 12

\$ Price

Total 0.00 EUR

Total: 0.00 EUR

[CLOSE WINDOW](#)[ORDER MORE](#)

Permission for re-use figure 7 and 8 in manuscript: Screenshot of Rightslink (obtained 13-03-2020)

SPRINGER NATURE

Amplitude-based optimal respiratory gating in positron emission tomography in patients with primary lung cancer

Author: Willem Grootjans et al
Publication: European Radiology
Publisher: Springer Nature
Date: Aug 6, 2014
Copyright © 2014, Springer Nature

Order Completed

Thank you for your order.

This Agreement between Willem Grootjans ("You") and Springer Nature ("Springer Nature") consists of your license details and the terms and conditions provided by Springer Nature and Copyright Clearance Center.

Your confirmation email will contain your order number for future reference.

License Number 4786981187203

[Printable Details](#)

License date Mar 13, 2020

Licensed Content

Licensed Content Publisher Springer Nature
Licensed Content Publication European Radiology
Licensed Content Title Amplitude-based optimal respiratory gating in positron emission tomography in patients with primary lung cancer
Licensed Content Author Willem Grootjans et al
Licensed Content Date Aug 6, 2014

Order Details

Type of Use Journal/Magazine
Requestor type non-commercial (non-profit)
Is this reuse sponsored by or associated with a pharmaceutical or a medical products company? no
Format electronic
Portion figures/tables/illustrations
Number of figures/tables/illustrations 2
Will you be translating? no
Circulation/distribution 200 - 499
Author of this Springer Nature content yes

About Your Work

Title of new article Management of respiratory motion artefacts in 18F-fluorodeoxyglucose positron emission tomography using an amplitude-based optimal respiratory gating algorithm
Lead author Willem Grootjans
Title of targeted journal Journal of Visualized Experiments
Publisher Journal of Visualized Experiments
Expected publication date May 2020

Additional Data

Portions Figure 3, page 3246 Figure 4, page 3248

Requestor Location

Willem Grootjans
Signapleinlaan 665Requestor Location
Leiden, 2321 KL
Netherlands
Attn: Willem Grootjans

Tax Details

\$ Price

Total 0.00 EUR

Total: 0.00 EUR

[CLOSE WINDOW](#)[ORDER MORE](#)

Permission for re-use figure 9 in manuscript: Screenshot of Rightslink (obtained 13-03-2020)



1 Alewife Center #200
Cambridge, MA 02140
tel: 617.945.9051
www.jove.com

ARTICLE AND VIDEO LICENSE AGREEMENT

Title of Article:

management of respiratory motion artefacts in ¹⁸F-FDG PET using amplitude-based optimal respiratory gating algorithm

Author(s):

W. Grootjans, P. Kok, J. Butter, E.H.J.G. Aarntzen

Item 1: The Author elects to have the Materials be made available (as described at <http://www.jove.com/publish>) via:

☒ Standard Access

☐ Open Access

Item 2: Please select one of the following items:

☒ The Author is **NOT** a United States government employee.

☐ The Author is a United States government employee and the Materials were prepared in the course of his or her duties as a United States government employee.

☐ The Author is a United States government employee but the Materials were NOT prepared in the course of his or her duties as a United States government employee.

ARTICLE AND VIDEO LICENSE AGREEMENT

1. **Defined Terms.** As used in this Article and Video License Agreement, the following terms shall have the following meanings: **"Agreement"** means this Article and Video License Agreement; **"Article"** means the article specified on the last page of this Agreement, including any associated materials such as texts, figures, tables, artwork, abstracts, or summaries contained therein; **"Author"** means the author who is a signatory to this Agreement; **"Collective Work"** means a work, such as a periodical issue, anthology or encyclopedia, in which the Materials in their entirety in unmodified form, along with a number of other contributions, constituting separate and independent works in themselves, are assembled into a collective whole; **"CRC License"** means the Creative Commons Attribution-Non Commercial-No Derivs 3.0 Unported Agreement, the terms and conditions of which can be found at: <http://creativecommons.org/licenses/by-nc-nd/3.0/legalcode>; **"Derivative Work"** means a work based upon the Materials or upon the Materials and other pre-existing works, such as a translation, musical arrangement, dramatization, fictionalization, motion picture version, sound recording, art reproduction, abridgment, condensation, or any other form in which the Materials may be recast, transformed, or adapted; **"Institution"** means the institution, listed on the last page of this Agreement, by which the Author was employed at the time of the creation of the Materials; **"JoVE"** means MyJoVE Corporation, a Massachusetts corporation and the publisher of The Journal of Visualized Experiments; **"Materials"** means the Article and / or the Video; **"Parties"** means the Author and JoVE; **"Video"** means any video(s) made by the Author, alone or in conjunction with any other parties, or by JoVE or its affiliates or agents, individually or in collaboration with the Author or any other parties, incorporating all or any portion

of the Article, and in which the Author may or may not appear.

2. **Background.** The Author, who is the author of the Article, in order to ensure the dissemination and protection of the Article, desires to have the JoVE publish the Article and create and transmit videos based on the Article. In furtherance of such goals, the Parties desire to memorialize in this Agreement the respective rights of each Party in and to the Article and the Video.

3. **Grant of Rights in Article.** In consideration of JoVE agreeing to publish the Article, the Author hereby grants to JoVE, subject to **Sections 4 and 7** below, the exclusive, royalty-free, perpetual (for the full term of copyright in the Article, including any extensions thereto) license (a) to publish, reproduce, distribute, display and store the Article in all forms, formats and media whether now known or hereafter developed (including without limitation in print, digital and electronic form) throughout the world, (b) to translate the Article into other languages, create adaptations, summaries or extracts of the Article or other Derivative Works (including, without limitation, the Video) or Collective Works based on all or any portion of the Article and exercise all of the rights set forth in (a) above in such translations, adaptations, summaries, extracts, Derivative Works or Collective Works and (c) to license others to do any or all of the above. The foregoing rights may be exercised in all media and formats, whether now known or hereafter devised, and include the right to make such modifications as are technically necessary to exercise the rights in other media and formats. If the "Open Access" box has been checked in **Item 1** above, JoVE and the Author hereby grant to the public all such rights in the Article as provided in, but subject to all limitations and requirements set forth in, the CRC License.

ARTICLE AND VIDEO LICENSE AGREEMENT

4. **Retention of Rights in Article.** Notwithstanding the exclusive license granted to JoVE in **Section 3** above, the Author shall, with respect to the Article, retain the non-exclusive right to use all or part of the Article for the non-commercial purpose of giving lectures, presentations or teaching classes, and to post a copy of the Article on the Institution's website or the Author's personal website, in each case provided that a link to the Article on the JoVE website is provided and notice of JoVE's copyright in the Article is included. All non-copyright intellectual property rights in and to the Article, such as patent rights, shall remain with the Author.

5. **Grant of Rights in Video – Standard Access.** This **Section 5** applies if the "Standard Access" box has been checked in **Item 1** above or if no box has been checked in **Item 1** above. In consideration of JoVE agreeing to produce, display or otherwise assist with the Video, the Author hereby acknowledges and agrees that, Subject to **Section 7** below, JoVE is and shall be the sole and exclusive owner of all rights of any nature, including, without limitation, all copyrights, in and to the Video. To the extent that, by law, the Author is deemed, now or at any time in the future, to have any rights of any nature in or to the Video, the Author hereby disclaims all such rights and transfers all such rights to JoVE.

6. **Grant of Rights in Video – Open Access.** This **Section 6** applies only if the "Open Access" box has been checked in **Item 1** above. In consideration of JoVE agreeing to produce, display or otherwise assist with the Video, the Author hereby grants to JoVE, subject to **Section 7** below, the exclusive, royalty-free, perpetual (for the full term of copyright in the Article, including any extensions thereto) license (a) to publish, reproduce, distribute, display and store the Video in all forms, formats and media whether now known or hereafter developed (including without limitation in print, digital and electronic form) throughout the world, (b) to translate the Video into other languages, create adaptations, summaries or extracts of the Video or other Derivative Works or Collective Works based on all or any portion of the Video and exercise all of the rights set forth in (a) above in such translations, adaptations, summaries, extracts, Derivative Works or Collective Works and (c) to license others to do any or all of the above. The foregoing rights may be exercised in all media and formats, whether now known or hereafter devised, and include the right to make such modifications as are technically necessary to exercise the rights in other media and formats. For any Video to which this **Section 6** is applicable, JoVE and the Author hereby grant to the public all such rights in the Video as provided in, but subject to all limitations and requirements set forth in, the CRC License.

7. **Government Employees.** If the Author is a United States government employee and the Article was prepared in the course of his or her duties as a United States government employee, as indicated in **Item 2** above, and any of the licenses or grants granted by the Author hereunder exceed the scope of the 17 U.S.C. 403, then the rights granted hereunder shall be limited to the maximum

rights permitted under such statute. In such case, all provisions contained herein that are not in conflict with such statute shall remain in full force and effect, and all provisions contained herein that do so conflict shall be deemed to be amended so as to provide to JoVE the maximum rights permissible within such statute.

8. **Protection of the Work.** The Author(s) authorize JoVE to take steps in the Author(s) name and on their behalf if JoVE believes some third party could be infringing or might infringe the copyright of either the Author's Article and/or Video.

9. **Likeness, Privacy, Personality.** The Author hereby grants JoVE the right to use the Author's name, voice, likeness, picture, photograph, image, biography and performance in any way, commercial or otherwise, in connection with the Materials and the sale, promotion and distribution thereof. The Author hereby waives any and all rights he or she may have, relating to his or her appearance in the Video or otherwise relating to the Materials, under all applicable privacy, likeness, personality or similar laws.

10. **Author Warranties.** The Author represents and warrants that the Article is original, that it has not been published, that the copyright interest is owned by the Author (or, if more than one author is listed at the beginning of this Agreement, by such authors collectively) and has not been assigned, licensed, or otherwise transferred to any other party. The Author represents and warrants that the author(s) listed at the top of this Agreement are the only authors of the Materials. If more than one author is listed at the top of this Agreement and if any such author has not entered into a separate Article and Video License Agreement with JoVE relating to the Materials, the Author represents and warrants that the Author has been authorized by each of the other such authors to execute this Agreement on his or her behalf and to bind him or her with respect to the terms of this Agreement as if each of them had been a party hereto as an Author. The Author warrants that the use, reproduction, distribution, public or private performance or display, and/or modification of all or any portion of the Materials does not and will not violate, infringe and/or misappropriate the patent, trademark, intellectual property or other rights of any third party. The Author represents and warrants that it has and will continue to comply with all government, institutional and other regulations, including, without limitation all institutional, laboratory, hospital, ethical, human and animal treatment, privacy, and all other rules, regulations, laws, procedures or guidelines, applicable to the Materials, and that all research involving human and animal subjects has been approved by the Author's relevant institutional review board.

11. **JoVE Discretion.** If the Author requests the assistance of JoVE in producing the Video in the Author's facility, the Author shall ensure that the presence of JoVE employees, agents or independent contractors is in accordance with the relevant regulations of the Author's institution. If more than one author is listed at the beginning of this Agreement, JoVE may, in its sole

ARTICLE AND VIDEO LICENSE AGREEMENT

discretion, elect not take any action with respect to the Article until such time as it has received complete, executed Article and Video License Agreements from each such author. JoVE reserves the right, in its absolute and sole discretion and without giving any reason therefore, to accept or decline any work submitted to JoVE. JoVE and its employees, agents and independent contractors shall have full, unfettered access to the facilities of the Author or of the Author's institution as necessary to make the Video, whether actually published or not. JoVE has sole discretion as to the method of making and publishing the Materials, including, without limitation, to all decisions regarding editing, lighting, filming, timing of publication, if any, length, quality, content and the like.

12. **Indemnification.** The Author agrees to indemnify JoVE and/or its successors and assigns from and against any and all claims, costs, and expenses, including attorney's fees, arising out of any breach of any warranty or other representations contained herein. The Author further agrees to indemnify and hold harmless JoVE from and against any and all claims, costs, and expenses, including attorney's fees, resulting from the breach by the Author of any representation or warranty contained herein or from allegations or instances of violation of intellectual property rights, damage to the Author's or the Author's institution's facilities, fraud, libel, defamation, research, equipment, experiments, property damage, personal injury, violations of institutional, laboratory, hospital, ethical, human and animal treatment, privacy or other rules, regulations, laws, procedures or guidelines, liabilities and other losses or damages related in any way to the submission of work to JoVE, making of videos by JoVE, or publication in JoVE or elsewhere by JoVE. The Author shall be responsible for, and shall hold JoVE harmless from, damages caused by lack of sterilization, lack of cleanliness or by contamination due to

the making of a video by JoVE its employees, agents or independent contractors. All sterilization, cleanliness or decontamination procedures shall be solely the responsibility of the Author and shall be undertaken at the Author's expense. All indemnifications provided herein shall include JoVE's attorney's fees and costs related to said losses or damages. Such indemnification and holding harmless shall include such losses or damages incurred by, or in connection with, acts or omissions of JoVE, its employees, agents or independent contractors.

13. **Fees.** To cover the cost incurred for publication, JoVE must receive payment before production and publication the Materials. Payment is due in 21 days of invoice. Should the Materials not be published due to an editorial or production decision, these funds will be returned to the Author. Withdrawal by the Author of any submitted Materials after final peer review approval will result in a US\$1,200 fee to cover pre-production expenses incurred by JoVE. If payment is not received by the completion of filming, production and publication of the Materials will be suspended until payment is received.

14. **Transfer, Governing Law.** This Agreement may be assigned by JoVE and shall inure to the benefits of any of JoVE's successors and assignees. This Agreement shall be governed and construed by the internal laws of the Commonwealth of Massachusetts without giving effect to any conflict of law provision thereunder. This Agreement may be executed in counterparts, each of which shall be deemed an original, but all of which together shall be deemed to be one and the same agreement. A signed copy of this Agreement delivered by facsimile, e-mail or other means of electronic transmission shall be deemed to have the same legal effect as delivery of an original signed copy of this Agreement.

A signed copy of this document must be sent with all new submissions. Only one Agreement is required per submission.

CORRESPONDING AUTHOR

Name:

E.H.J.G. AARNTZEN

Department:

RADIOLOGY AND NUCLEAR MEDICINE

Institution:

RADBOUD UNIVERSITY MEDICAL CENTER

Title:

MD, PhD

Signature:



Date:

OCTOBER 23rd 2019

Please submit a **signed** and **dated** copy of this license by one of the following three methods:

1. Upload an electronic version on the JoVE submission site
2. Fax the document to +1.866.381.2236
3. Mail the document to JoVE / Attn: JoVE Editorial / 1 Alewife Center #200 / Cambridge, MA 02140